BIOCHEMICAL PHARMACOLOGY 71 (2006) 319–337

available at www.sciencedirect.com

SCIENCE DIRECT®

journal homepage: www.elsevier.com/locate/biochempharm

Identification and characterization of surrogate peptide ligand for orphan G protein-coupled receptor mas using phage-displayed peptide library

Rama Kamesh Bikkavilli [a], *Sup-Yin Tsang* [a], *Wai-Man Tang* [a], *Jing-Xin Sun* [a], *Sai-Ming Ngai* [c], *Susanna Sau-Tuen Lee* [a], *Wing-Hung Ko* [d], *Helen Wise* [b], *Wing-Tai Cheung* [a,*]

[a] *Department of Biochemistry, The Chinese University of Hong Kong, Shatin, New Territories, Hong Kong, China*
[b] *Department of Pharmacology, The Chinese University of Hong Kong, Shatin, New Territories, Hong Kong, China*
[c] *Department of Biology, The Chinese University of Hong Kong, Shatin, New Territories, Hong Kong, China*
[d] *Department of Physiology, The Chinese University of Hong Kong, Shatin, New Territories, Hong Kong, China*

ARTICLE INFO

Article history:
Received 9 August 2005
Accepted 31 October 2005

Keywords:
Angiotensin
GPCR
Mas
Oncogene
Peptide library
Phage display

ABSTRACT

In the present study, a phage-displayed random peptide library was used to identify surrogate peptide ligands for orphan GPCR mas. Sequence analysis of the isolated phage clones indicated a selective enrichment of some peptide sequences. Moreover, multiple alignments of the isolated phage clones gave two conserved peptide motifs from which we synthesized peptide MBP7 for further evaluation. Characterization of the representative phage clones and the synthetic peptide MBP7 by immunocytochemistry revealed a strong punctate cell surface staining in CHO cells expressing mas-GFP fusion protein. The isolated phage clones and synthetic peptide MBP7 induced mas internalization in a stable CHO cell clone (MC0M80) over-expressing mas. In addition, MBP7-stimulated phospholipase C activity and intracellular calcium mobilization in these same cells. In summary, we have demonstrated a systematic approach to derive surrogate peptide ligands for orphan GPCRs. With this technique, we have identified two conserved peptide motifs which allow us to identify potential protein partners for mas, and have generated a peptide agonist MBP7 which will be invaluable for functional characterization of the mas oncogene.

1. Introduction

G protein-coupled receptors (GPCRs) constitute the single largest and the most diverse family of receptors, and they are characterized with seven distinct hydrophobic regions and are known to be activated by a diverse array of extracellular ligands. In the last decade, the progress in genome sequencing has led to the discovery of new GPCR family members, and over 1000 GPCRs have been cloned from a wide range of species. Many of the novel receptors identified have no known ligand and are classified as orphan receptors. Indeed, 50% of the cloned GPCRs are orphan receptors [1]. The challenge ahead is to characterize these orphan receptors by identifying their cognate/surrogate ligands and unraveling their biological roles.

Mas oncogene was identified by a tumorigenicity assay in which NIH3T3 cells were transfected with DNA from an epidermoid carcinoma [2]. Mas was predicted to be a GPCR and

* *Corresponding author*. Tel.: +852 2609 6104; fax: +852 2603 7246.
E-mail address: wtcheung@cuhk.edu.hk (W.-T. Cheung).
0006-2952/$ – see front matter
doi:10.1016/j.bcp.2005.10.050

has been demonstrated to be abundantly expressed in the brain and the testis [3,4]. Activation of mas proto-oncogene results from a 5′-rearrangement while there is no nucleotide change in the coding region [2]. Similar findings were also reported in an ovarian carcinoma [5] and an acute leukaemia [6].

Phage-displayed random peptide libraries provide a good source of epitopes that could potentially function as surrogate ligands for many receptors. To construct a phage-displayed random peptide library, a pool of small random peptide epitopes are tagged to the N-terminus of M13 phage gIII coat proteins which are expressed on the phage surface [7]. Peptide sequences that have high affinity to the target receptor are commonly selected against immobilized targets by a process of repeated binding and elution cycles known as panning. The major shortcoming of using immobilized targets or fixed cells for panning is of retrieving epitopes that might not bind to the native receptor [8]. On the other hand, live cell panning facilitates the selection of functionally active ligands that recognize the native receptors [9,10].

In the present study, we used a phage-displayed 12-mer random peptide library to identify surrogate peptides of mas that were biologically active. Initially, we enriched peptides with consensus motifs by panning a phage library against live cells that were transiently expressing mas-GFP fusion protein. A synthetic peptide MBP7 with consensus motif was identified as an agonist for mas through stimulation of mas internalization, activation of phospholipase C (PLC), and intracellular calcium mobilization in a stable cell line that over-expressed mas. To our best understanding, this is the first report identifying a peptide agonist for an orphan G protein-coupled receptor using a phage-displayed random peptide library.

2. Materials and methods

2.1. Materials

The rabbit anti-mas receptor polyclonal antibody was raised against a putative C-terminal peptide of the mas protein (RAFKDEMQPRRQKDNC) using standard techniques as described previously [11]. SuperScript II, T4 DNA ligase, Iscove's modified DMEM medium, fetal bovine serum, penicillin/streptomycin, HT supplement, trypsin, TRIzol™ reagent, mas peptide antigen and various oligos were from Invitrogen (Carlsbad, CA, USA). The MBP7 (KAQLRRLS) peptide was synthesized in-house using Fmoc solid-phase technique with an Applied Biosystems 433A peptide synthesizer (Applied Biosystems, Foster City, CA, USA). Cy^3-conjugated sheep anti-mouse antibody and FITC-conjugated sheep anti-rabbit antibody were from Zymed Laboratories (San Francisco, CA, USA). Alexa Fluor 546 succinimidyl ester was from Molecular Probes (Eugene, OR, USA). pBluescript vector was from Stratagene (La Jolla, CA, USA). pCANTAB 5E phagemid vector, ATP, and HRP-conjugated anti-M13 antibody were from Amersham Biosciences (GE Healthcare Ltd., Piscataway, NJ, USA). pFRSV vector was a generous gift from Dr. Shawn S.O. Leung. All the restriction enzymes were from New England Biolabs (Beverley, MA, USA). QIAquick gel extraction kit, Qiagen plasmid midi and maxi kits were from Qiagen (Hilden, Germany). Wizard plus minipreps and Geneclean II kit were from Promega (Madison, WI, USA). Dye-labeled terminator cycle sequencing kit was from Beckman Coulter (Fullerton, CA, USA). [^{3}H]-*myo*-Inositol was purchased from NEN Life Sciences Products (Boston, MA, USA). DIG easy hybridization buffer solution, blocking reagent, nitroblue tetrazolium chloride (NBT), 5-bromo-4-chloro-3-indolyl-phosphate-4-toludine salt (BCIP), digoxigenin-11-2′-deoxyuridine-5′-triphosphate (DIG-11-UTP), anti-digoxigenin-AP (Fab fragments), and DIG-RNA molecular weight marker I (0.3–6.9 kb) were from Roche Diagnostics (Roche Diagnostics Corporation, Indianapolis, IN, USA). The membrane permeant acetoxymethylester (AM) forms of Fura-2 and pluronic F127 were obtained from Molecular Probes. All the other chemicals and reagents of highest grade were from Sigma (St. Louis, MO, USA).

2.2. Construction of stable cell lines over-expressing mas

The cell stock of Chinese hamster ovary cells deficient in dihydrofolate reductase (CHO Dhfr$^-$) was obtained from the American Type Culture Collection (ATCC, Rockville, MD, USA), and the cells were cultured in Iscove's modified DMEM medium (IMDM) supplemented with hypoxanthine and thymidine (HT) as recommended by ATCC.

Full-length mas cDNA was obtained by RT-PCR as described previously [12]. Briefly, total RNA (5 μg) extracted from AR4-2J cells was reversely transcribed into cDNA with Superscript II RNase H$^-$ in a reaction volume of 20 μl. One-tenth of the reverse transcription product was used for PCR in a reaction volume of 50 μl containing 5 U of Taq polymerase, 1× PCR buffer, 1 mM $MgCl_2$, 0.2 mM dNTP, and 1 μM each of forward and reverse primers of 5′-TCATGGACCAATCAAATATGACATCC-3′ and 5′-TCCTCAGACCACAGTCTCAATGGAT-3′, respectively. After an initial denaturation at 94 °C for 3 min, the PCR was carried out with a denaturation temperature at 94 °C for 30 s, an annealing temperature at 58 °C for 60 s and an extension temperature at 72 °C for 60 s for 30 cycles followed by an extended incubation at 72 °C for 5 min. After gel extraction and purification with Geneclean II, the PCR product was cloned into pBluescript II KS vector at the EcoRV site by TA cloning. Nucleotide sequence of the full-length mas clone was confirmed by DNA sequencing. The full-length mas cDNA was then sub-cloned at the *Eco*RI restriction site of the pFRSV plasmid to create pFRSV/mas that harbored a dihydrofolate reductase (DHFR) gene as a selection marker. For generation of stable cell lines over-expressing mas, the pFRSV or pFRSV/mas plasmids were electroporated into CHO Dhfr$^-$ cells in a 0.8 ml electroporation cuvette (4 mm gap, 450 V, 25 μF for 0.5 ms). The transformants were selected in IMDM supplemented with 10% dialyzed FBS. After 14 days, the resistant colonies were spotted and isolated using cloning cylinders. After confirming the expression of mas by RT-PCR, a clone (MC0) was selected and amplification of the mas transgene was accomplished by step-wise increase of methotrexate (MTX) in selection medium from a concentration of 0.05 to 80 μM over a period of 3 months. The resulting stable cell line (MC0M80) was cultured in selection medium supplemented with 80 μM MTX. The control cell clone, VC0M80, was transfected with pFRSV vector and underwent the same MTX treatment as MC0M80 cells.

2.3. Transient and stable expression of mas-GFP fusion protein

The mas-GFP fusion protein construct was created by amplifying the full-length mas cDNA from pFRSV/mas with a 3′-primer that mutated the stop codon (TGA) of mas to glycine (GGA) and then sub-cloning into the pEGFP-N1 vector at the *Eco*RI and *Kpn*I sites. The nucleotide sequence of mas-GFP fusion protein construct was confirmed by DNA sequencing.

For transient expressions, CHO Dhfr$^-$ cells (1×10^5 cells/well in a six-well plate) were transfected with 4 μg of the plasmid DNA in 1 ml of serum-free DMEM medium containing 6 μg of lipofectamine for 3 h followed by a post-transfection incubation in normal culture medium with serum at 37 °C for 24 h. For generation of the stable cell lines expressing mas-GFP, the cells were selected in IMDM supplemented with 10% FBS, 1% penicillin and streptomycin, 1× HT (0.1 mM sodium hypoxanthine and 0.016 mM thymidine), and 1 mg/ml G418. Cell clones expressing mas-GFP fusion protein were isolated by two successive sub-clonings (cloning cylinders followed by limiting dilutions). The stable cell lines (Mas-GFP-Sc9 and Mas-GFP-Sc11) generated were cultured in selection medium supplemented with 500 μg/ml G418 at 37 °C in a humidified atmosphere containing 5% CO_2. Cell clones transfected with pEGFP-N1 vector and expressing GFP were used as controls.

2.4. Construction of phage-displayed random peptide library

A random peptide library displaying 12 amino acids was generated by a PCR based method. Briefly, a template oligonucleotide was custom synthesized with sequence as: 5′-ATCGAACTGTCT(NNS)$_{12}$AAGCAGAATGC-3′ where N = A, T, G or C and S = G or C. The random peptide library was then generated by PCR amplification of the template oligo with a pair of adapter oligos that have nucleotide sequences as: 5′-GGGGTACCCCGGCCCAGCCGGCCATCGAACTGTCT-3′ and 5′-ATAGCGATGCGGCCGCATTCTGCTT-3′. The forward and reverse adapter oligos contained a *Sfi*I and a *Not*I restriction sites (underlined sequences in the primers), respectively. A two-step PCR was carried out with a denaturation temperature at 94 °C for 30 s and an annealing/extension temperature at 70 °C for 30 s for 25 cycles. The resulting 101 bp PCR product was digested with *Bgl*I (gives the same cohesive end as *Sfi*I) and *Not*I, ethanol precipitated and was further purified using CHROMA SPIN^{TM} 30 TE column (Clontech, Palo Alto, CA, USA). The purifed insert (70 bp) was ligated to pCANTAB 5E phagemid (linearized with *Sfi*I and *Not*I) at 16 °C overnight. The ligation product was ethanol precipitated and electroporated into *E. coli* at 2500 V, 50 μF, and 400 Ω in an electroporation cuvette (0.2 mm gap; 0.4 ml volume) containing 10 μg DNA and 100 or 400 μl of *E. coli* strain TG1 electrocompetent cells with a gene pulser (Bio-Rad, Hercules, CA, USA). The resultant library was amplified by culturing the library in 200 ml of 2× YT medium with respective antibiotics at 37 °C for 5 h and 10 aliquots were made. The diversity of the library was estimated by counting the colony forming units (cfu) and the characteristics of the library was studied by sequencing randomly selected clones (30 clones). The recombinant filamentous M13 phage library for screening was produced by rescue of the library using M13KO7 helper phage as recommended by the manufacturer (Amersham).

2.5. Phage-displayed random peptide library screening

The phage-displayed random peptide library was biopanned against CHO Dhfr$^-$ cells transiently expressing (24 h) mas-GFP fusion protein in a six-well plate by incubating with 2 ml of rescued phage for 2 h at 37 °C. The non-specific phage binding to the cells were depleted from the library by pre-incubating the library with CHO Dhfr$^-$ cells transiently expressing GFP protein for 2 h at 37 °C prior to the addition to mas-GFP expressing cells. After incubation of phage with the cells transiently expressing mas-GFP, the supernatant was aspirated and the cells were washed 20 times in Hank's balanced salt solution. The specifically bound phage were first eluted with 1 ml of an acid elution buffer (0.1N HCl adjusted with concentrated glycine to pH 2.2) for 5 min at room temperature followed by quick neutralization with 100 μl of 1 M Tris–HCl (pH 8.0) (acid eluate fraction). Phages that are tightly associated with cells were recovered by lysis of collected cells in 100 μl of Hank's solution with 1% Tween-20 (detergent eluate fraction). Phages for the next round of selection were prepared by infection of the *E. coli* TG1 with the pooled eluted fractions (acid eluate and detergent eluate) and rescued with 4×10^{12} pfu of M13KO7 helper phage (multiplicity of infection-5). After overnight growth at 37 °C, the supernatant containing the phage particles was precipitated with 20% PEG/NaCl (20% polyethylene glycol 8000 and 2.5 M NaCl), mixed vigorously and incubated on ice for 1 h. The precipitated phages were then collected by centrifugation at 10,000 × *g* for 15 min at 4 °C. The phage pellet was resuspended in 2 ml of Iscove's modified DMEM supplemented with 10% FBS and 0.1% BSA for use in the subsequent rounds of selection. A total of five selection cycles were performed. The performance of the panning was evaluated by plating an aliquot of the recovered phage after each round of panning. Furthermore, the acid eluate and detergent eluate fractions of the fifth round were plated separately for analysis.

2.6. PhageELISA

The binding activity of selected phage clones were initially evaluated by a phageELISA. Briefly, individual single colonies were randomly picked and inoculated into 2× YT medium (500 μl/well) containing 2% glucose and 100 μg/ml of ampicillin in a 96-well cluster plate (Corning, Acton, MA, USA, 2 ml assay block) and incubated at 37 °C overnight with shaking (master plate). To rescue the phage from the individual clones, replicas of the master plates were prepared by adding 60 μl of overnight culture from the master plate to 540 μl/well of M13KO7 helper phage suspension (2× YT medium supplemented with 6×10^8 pfu/ml of M13KO7, 100 μg/ml ampicillin, and 2% glucose) in a 96-well cluster plate. The phage infection was performed by incubating the replica plate at 37 °C with shaking at 250 rpm for 2 h. After 2 h, the infected bacterial cells were collected by centrifugation at 2750 × *g* for 5 min at room temperature in an Eppendorf 5810 centrifuge (Eppendorf AG, Hamburg, Germany) equipped with a swing-bucket rotor (A-4-

62) with carriers for 96-well microtiter plates. The medium was then quickly discarded and cells in each well were resuspended in 600 μl of 2× YT medium containing 100 μg/ml ampicillin and 50 μg/ml of kanamycin. The culture was incubated overnight at 37 °C with shaking at a rotation rate of 250 rpm. The next day, culture was centrifuged at 2750 × *g* for 5 min at room temperature and the phage supernatant was directly used for testing the phage binding by ELISA. Phage supernatants (100 μl/well) were added to CHO Dhfr$^-$ cells (2.5×10^4 cells/well in 96-well plates) stably expressing GFP or mas-GFP fusion protein, in duplicate, and incubated for 1 h at 37 °C. The wells were washed three times with IMDM medium supplemented with 10% FBS. Bound phages were detected with a peroxidase-conjugated anti-M13 antibody (Amersham, 1:3000 dilution in IMDM with FBS) and *o*-phenylenediamine (OPD) was used as substrate. After 1 h, the absorbance was measured at 450 nm using a microplate reader (μQuant, Bio-Tek Instruments, Winooski, VT, USA). Phagemids of the positive clones were subjected to dye terminator sequencing with a Beckman CEQ 2000 DNA sequencer as per the vendor's recommendation. The nucleotide sequences were translated into amino acid sequences in frame with respect to the gIII phage coat protein, and were manually aligned to determine the consensus regions.

2.7. Peptide synthesis and labeling

The peptides were either in-house or custom synthesized (Invitrogen). Purity of the peptides was evaluated by reverse phase HPLC, and peptide sequences were further confirmed by MALDI-ToF/ToF mass spectrometry (Applied Biosystems 4700 Proteomics Analyzer). The peptide MBP7 was conjugated to Alexa Fluor 546 by mixing 0.6 μM of succinimidyl ester with 20 μg of peptide in 100 mM sodium bicarbonate buffer, pH 8.3, followed by incubation at 4 °C with rocking for 16 h. After 16 h, the reaction was terminated by the addition of Tris–HCl, pH 8.0 (40 mM final concentration). Crude mixtures (50 μl) were injected onto a reversed phase analytical C18-column (C18, 10 μm, 4.6 mm × 250 mm; VyDAC, The Separations Group Inc., Hesperia, CA, USA) and the conjugated peptides were separated with a linear gradient of 0–60% acetonitrile containing 0.1% trifluoroacetic acid in H_2O as the mobile phase for 85 min at 1 ml/min. Elution of Alexa Fluor-conjugated peptide was monitored in series with an UV detector (Waters 486) and a fluorescence detector (LC-4C, Bioanalytical Systems Inc., West Lafayette, IN, USA) which were coupled to a chart recorder (NGI servogor 120, NGI Norma Goerz Instruments GmbH, Österreich, Austria). The eluted Alexa Fluor 546-conjugated peptide was further confirmed by MALDI-ToF/ToF analysis. Fractions of the purified Alexa Fluor 546-conjugated peptide (from five reactions) were pooled, lyophilized and the peptide was re-dissolved in 500 μl of water and stored at 4 °C until use.

2.8. Cell binding studies with isolated phage clones and Alexa Fluor 546-labeled MBP7

Cells (2.5×10^4) were grown on coverslips in a 24-well plate and phages ($\sim 2.5 \times 10^{12}$ phage particles) were added to the cells followed by incubation for 1 h at 37 °C. After washing the cells three times with IMDM supplemented with 10% FBS, the cells were fixed with 4% paraformaldehyde in PBS for 10 min followed by permeabilization with 0.05% IGEPAL CA-630 for another 10 min at room temperature. The cells were then incubated for 1 h with mouse monoclonal anti-M13 antibody (1:250 in IMDM with 10% FBS) at 37 °C followed by three washes with IMDM supplemented with 10% FBS. Finally the bound phage were detected by incubation with a Cy^3-conjugated sheep anti-mouse IgG (1:250) secondary antibody for 1 h. After air-drying, the coverslips were mounted with an anti-fade mounting medium and sealed with nail polish.

For co-staining of phage and mas protein, MC0M80 cells (2.5×10^4 cells/well) were incubated with $\sim 2.5 \times 10^{12}$ phage particles (3p5A190) for 5, 10, 15 and 20 min. The cells were then washed quickly, fixed and permeabilized as mentioned before. The mas protein and recombinant M13 phage were simultaneously detected with a rabbit polyclonal anti-mas peptide antibody (1:50) and a mouse monoclonal anti-M13 antibody (1:250) in DMEM medium supplemented with 10% FBS by incubating at 37 °C for 3 h. The cells were washed with PBS and incubated with a FITC-conjugated goat anti-rabbit IgG (1:250) and a Cy^3-conjugated sheep anti-mouse antibody (1:250) in DMEM supplemented with 10% FBS for 2 h at 37 °C. After washing the cells three times with PBS, coverslips were mounted with an anti-fade mounting medium and sealed with nail polish.

For internalization experiments with peptides, MC0M80 cells (2.5×10^4 cells/well) were incubated with MBP7 (10 μM) for 15 min at 37 °C and cellular distribution of the mas protein was localized by probing with the polyclonal anti-mas peptide antibody as described before.

For binding studies with the labeled peptide, CHO Dhfr$^-$ cells transiently transfected (24 h) with pEGFP-N1/mas were incubated with the Alexa Fluor 546-labeled MBP7 (1:25 dilution of the pooled fractions in IMDM supplemented with 10% FBS) at 37 °C for 30 min. After washing three times with IMDM supplemented with 10% FBS, the cells were fixed with 4% paraformaldehyde in PBS and then examined by confocal microscopy.

2.9. Confocal microscopy

Fluorescent staining of cell was visualized using a Leica confocal laser scanning microscope equipped with an argon/krypton laser as described previously [12]. The GFP and FITC were excited at 488 nm and fluorescent emission was detected with a 525/50 bandpass filter. The Cy^3 and Alexa Fluor 546 were excited at 568 nm and fluorescent emission was detected with a 600/50 bandpass filter. Serial scan was also performed to check for the channel cross-over. The captured images were processed for publication by Adobe Photoshop 6.0 (Adobe Systems, Mountain View, CA, USA).

2.10. Northern blot analysis

Total RNA was extracted from different cell lines using TRIzol™ reagent according to the manufacturer's recommendation, then dissolved in formamide and stored at −70 °C until use. The RNA was separated on 1% formaldehyde gel under constant voltage. The RNA was then transferred to Nylon

membrane (Hybond N^+, Amersham Biosciences) by upward capillary transfer and hybridized with DIG-labeled full-length mas probe at 42 °C in DIG-Easy Hyb buffer for 15–16 h. The DIG-labeled probe was prepared by a PCR method using PCR DIG-labeling mix (Roche). Briefly, the PCR mixture included the pFRSV/mas template (40 ng), 1× PCR buffer, 1.5 mM $MgCl_2$, 2.5 μl of PCR DIG-labeling mix, 1 μM each of forward primer (5′-CCGGAATTCATGGACCAATCAAATATGAC-3′) and reverse primer (5′-CCGGTACCCCTCCTCCGACCACAGTCTCA-3′) and 2.5 U of Taq polymerase in a final volume of 25 μl. The PCR was carried out with a denaturation temperature at 94 °C for 30 s, an annealing temperature at 65 °C for 30 s and an extension temperature at 72 °C for 90 s for 25 cycles followed by an extended incubation at 72 °C for 5 min. After hybridization, the membrane was then washed twice at room temperature with 2× SSC/0.1% SDS for 10 min followed by two washes with 0.5× SSC/0.1% SDS for 15 min at 65 °C. The membrane was finally developed by incubating with alkaline phosphatase conjugated anti-DIG antibody (1:10,000) in blocking reagent (Roche) for 1 h followed by incubation with the alkaline phosphatase substrate nitroblue tetrazolium chloride (NBT)/5-bromo-4-chloro-3-indolyl-phosphate-4-toludine salt (BCIP) until the bands were clearly visible. For normalization of sample loading and transfer of RNA, the blots were stripped and re-probed with a 306-bp (783–1088 bp of GAPDH, GenBank accession no. X52123) DIG-labeled glyceraldehyde 3-phosphate dehydrogenase (GAPDH) probe.

2.11. [^{3}H]-Inositol phosphate accumulation assay

[^{3}H]-Inositol phosphate ([^{3}H]-IP) accumulation was assayed in 12-well plates following 42 h incubation of cells with [^{3}H]-*myo*-inositol (2 μCi/ml: specific activity 10–25 Ci/mmol) as described previously [13]. Briefly, cells were washed twice with 1 ml of HEPES-buffered saline (HBS: 15 mM HEPES, pH 7.4, 140 mM NaCl, 4.7 mM KCl, 2.2 mM $CaCl_2$, 1.2 mM $MgCl_2$, 1.2 mM KH_2PO_4, 11 mM glucose), followed by 10 min incubation at 37 °C in HBS containing 20 mM LiCl. The buffer was removed and replaced with fresh buffer and the cells were incubated in the absence or presence of various combinations of MBP7 and ATP at the indicated concentrations for a further 60 min. The reaction was terminated by aspiration and addition of ice-cold 20 mM formic acid. [^{3}H]-Inositol phosphates were separated from the [^{3}H]-inositol fraction by column chromatography. For analysis of log concnetration–response curves, normalized data sets were curve fitted with non-linear regression using Prism 4 (GraphPad Software, Inc., San Diego, CA, USA).

2.12. Measurement of intracellular free Ca^{2+} ($[Ca^{2+}]_i$)

The changes in $[Ca^{2+}]_i$ were monitored using standard microspectrofluorimetric techniques as described previously [14]. Briefly, agonist-induced calcium signals were measured in CHO cells grown on glass coverslips. Cells were loaded with 3 μM Fura-2/AM and 1.6 μM pluronic F127 for 45 min at 37 °C in bicarbonate-buffered Krebs–Henseleit (K–H) solution contained 117 mM NaCl, 25 mM $NaHCO_3$, 4.7 mM KCl, 1.2 mM $MgSO_4$, 1.2 mM KH_2PO_4, 2.5 mM $CaCl_2$, and 11 mM D-glucose, pH 7.4 when bubbled with 5% CO_2/95% O_2. After being washed, the coverslips were mounted in a chamber attached to the stage of an inverted microscope (Nikon TE300, Nikon Corporation, Tokyo, Japan). The cells were viewed with a 40× objective (Nikon CFI S Fluor 40× oil, 1.3 numerical aperture). Fura-2 fluorescence ratios (excitation wavelength 340 and 380 nm; emission wavelength > 510 nm) were recorded from three to five cells at 20 Hz (PTI Ratio-Master fluorescence system, Photon Technology International, Birmingham, NJ, USA) at room temperature. Increase in $[Ca^{2+}]_i$ was represented by changes (Δ) in Fura-2 fluorescence ratio quantified by measuring the fluorescence ratio at the peak of a response and subtracting from it the ratio measured before stimulation. Pooled data are presented as means ± standard errors (S.E.), and values of n refer to the number of experiments in each group.

3. Results

3.1. Characteristics of the phage-displayed random peptide library

A random peptide library displaying 12 amino acids was constructed by cloning the PCR amplified oligo templates upstream and inframe to the M13 phage coat protein gIII. The resultant library comprised more than 2.2×10^9 recombinants and 30 clones were randomly selected for analysis. Analysis of the nucleotide sequences of the 30 inserts showed that the random peptide library was predominantly in accordance with the NNS pattern and there was no bias towards any particular nucleotides (Fig. 1A). However, a lower representation of nucleotide A in the first and second positions and the presence of nucleotides A and T in the third position of the codon were observed in the randomly selected phage clones. Furthermore, it was also observed that some inserts displayed more than 12 amino acids in the peptide coding region, ranging form 11 to 16 amino acid residues (Fig. 1B). These irregularities may result from sliding of the adapter primers during PCR amplification of template oligo. The amino acid sequences were deduced by translating the random peptide encoding insert region. Since the library was harbored in a *SupE* bacterial strain, the amber stop codon (UAG) was read by incorporating glutamine at that position. Also, as UGA codon is the least efficient termination codon, it was read by incorporating tryptophan [15]. The distribution of the individual amino acids in the library was broadly in accordance with the expected amino acid distribution frequencies (Fig. 1C) except for the amino acids glutamine and tryptophan which were over-represented, and for lysine and tyrosine which were under-represented. The over-representation of the glutamine and tryptophan resulted from the usage of these amino acids for reading the UAG and UGA stop codons, while the under-representation of lysine and tyrosine was attributed to a lower representation of nucleotide A in the first and second positions of the codon. Despite these observations, the random peptide library still represented as a pool of heterogeneous peptides with sufficient diversity in amino acid composition.

3.2. Characteristics of mas expressing cell lines

The cDNA encoding the full-length GPCR mas was cloned into two different expression vectors, namely pFRSV and pEGFP-

Base	Codon Position		
	1	2	3
A	18.7% (70)	20.4% (77)	3.9% (15)
T	27.3% (103)	28.1% (106)	5.8% (22)
G	26.1% (98)	26.6% (100)	44.9% (169)
C	27.9% (105)	24.7% (93)	45.2% (170)

(A)

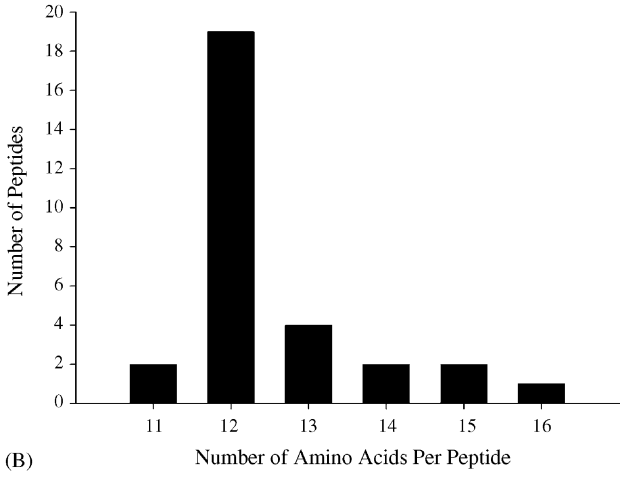

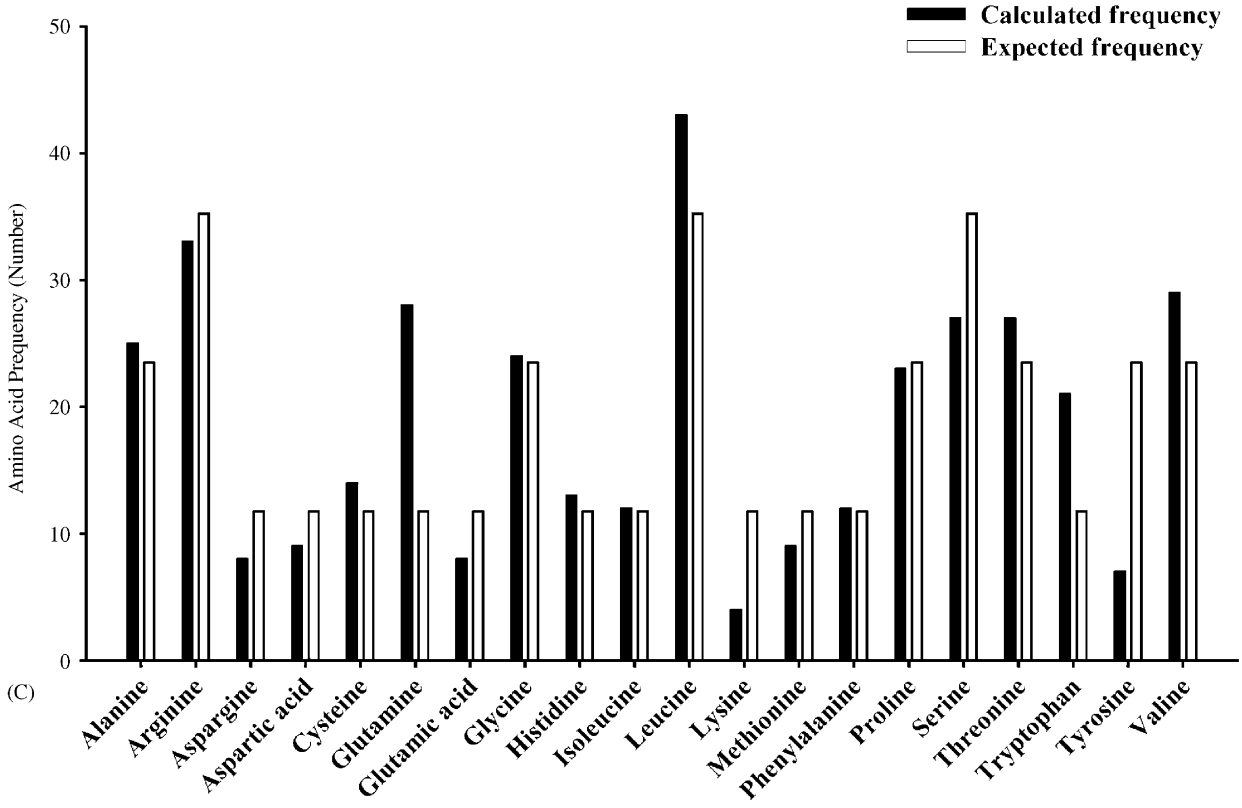

Fig. 1 – Characteristics of the random peptide library. (A) Nucleotide distribution of 30 randomly selected clones at each position of the codons that encoded the random peptides. Actual number of each nucleotide at each position of the codons was shown in parentheses. (B) Distribution of peptide length among the 30 randomly selected phage clones. (C) Frequency of the individual amino acid distributions in the 30 randomly selected inserts. The observed frequency of each amino acid was determined by counting the number of the amino acid in the pool. The expected frequency of each amino acid was calculated by multiplying the fraction of the codons that encode the amino acid by the total number of the amino acids in the pool.

N1, to obtain two different mas expression systems with different characteristics. Live cell imaging of the cell lines expressing mas-GFP fusion protein revealed the expression of the fusion protein which was predominantly on the cell surface suggesting mas is an integral membrane protein (Fig. 2C). Characterization of cells over-expressing mas (MC0M80) was performed by utilizing a polyclonal peptide antibody raised against the putative C-terminal tail of mas. Immunostaining of MC0M80 cells with the antibody revealed a dense staining (Fig. 2F), while only background fluorescence was observed in wild-type and VC0M80 cells (Fig. 2D and E). Furthermore, the antibody staining could be blocked by the peptide antigen that was used for raising the antibody, indicating the specificity of the antibody to mas (Fig. 2I). The

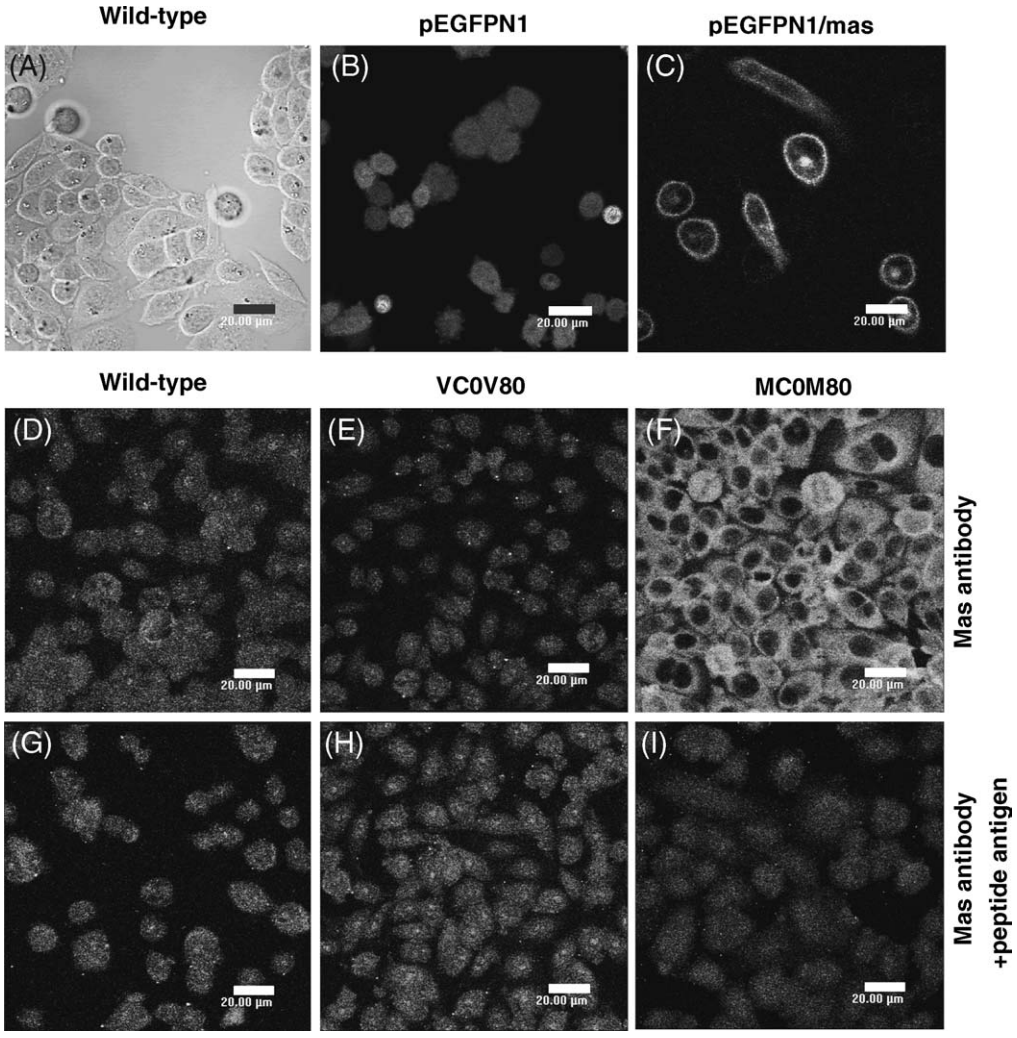

Fig. 2 – Characteristics of the mas expressing cell lines. Confocal images of wild-type CHO Dhfr$^-$ cells (A), cells stably expressing GFP (B) and mas-GFP (C). Mas-GFP fusion proteins were located predominantly on the membrane. Expression of native mas protein in transfected cells were examined by immunocytochemical methods with a rabbit polyclonal antibody against a peptide antigen that is derived from the putative C-terminal tail of mas. The wild-type CHO Dhfr$^-$, vector-transfected VC0M80 and mas over-expressing MC0M80 cells were immunostained with the anti-mas serum in the absence (D–F) and presence (G–I) of the peptide antigen (50 μg/ml). The anti-mas serum selectively stained the MC0M80 cells (panel F), and the staining could be completely blocked by the peptide antigen used for raising the antibody (panel I). Background staining was observed in wild-type and VC0M80 cells (panels D and E). The data shown represent three independent experiments with similar results. Scale bar, 20 μm.

two expression systems indicated clearly the expression of mas and also their suitability as good sources of mas for screening. In order to evaluate the mas-expression systems, Northern blotting was performed using a DIG-labeled full-length mas cDNA probe. The blot revealed a 1800 bp transcript in the stable mas-GFP-Sc11 cells expressing mas-GFP and a 4700 bp transcript in stable MC0M80 cells over-expressing mas (Fig. 3). It was also observed that the expression of mas transcripts was higher under a CMV promoter in pEGFP-N1 vector than under RSV promoter in pFRSV vector. In the transient expression system, in addition to the mas and mas-GFP transcripts that were observed in stable cells, transcripts characterized with a higher molecular mass corresponding to the complete transcription of the vectors (Fig. 3, marked with asterisk) were also detected. It is also noted that transient transfection of pEGFP-N1/mas for 24 h gave the highest expression of mas (Fig. 3), and hence transiently transfected cells were used for panning with the phage-displayed random peptide library.

3.3. *Identification of surrogate peptides binding to mas oncogene*

In the course of panning, changes in phage selection were monitored by the phage input/output ratio. The eluted phage titers remained stable during the first three rounds of panning, but a drastic decrease in eluted phage titer was noted in the fourth and the fifth rounds of panning (Fig. 4A). In order to evaluate the effectiveness of panning, randomly selected individual clones from the third, fourth and fifth rounds of panning were screened by phageELISA against stable cell lines

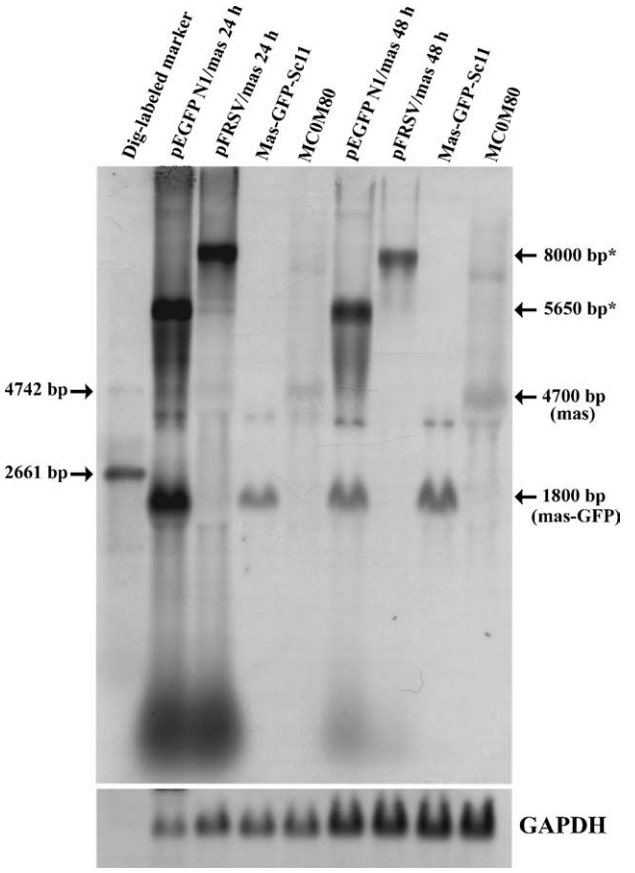

Fig. 3 – Northern blot analysis of mas expression. Total RNA in an amount of 10 μg (lanes 2–5) and 20 μg (lanes 6–9) was separated on formaldehyde agarose gels and Northern blotting was performed as described in Section 2. Mas expression was detected in all of the cell lines with different expression levels. Arrows indicate the sizes of RNAs. Asterisks indicate transcripts that are possibly derived from complete transcription of the vectors. The blot was de-probed and re-probed with glyceraldehyde 3-phosphate dehydrogenase (GAPDH) to normalize the loading and transfer.

expressing either GFP or mas-GFP (Fig. 4B). In total, 480 clones from different rounds of panning were screened and 295 clones were found to show ≥20% binding over their corresponding controls which were considered to be putative mas binding clones. The inserts of 92 positive clones were sequenced.

Sequence analysis of the 92 phage clones indicated that 56 clones gave three identical sequences, 27 clones contained at least a non-suppressed stop codon like UGA, and 58 clones contained one or two extra nucleotides in the region encoding the random peptides. Phage clones containing non-suppressive stop codons have been reported previously [16]. Since there was recombinant phage production by these clones as evidenced by their cell binding activities in phageELISA, all the clones that possess UAG and UGA were read by incorporating glutamine and tryptophan, respectively, as described earlier [15]. Clones that gave extra nuncleotides were translated such that the peptide sequences were aligned inframe with respect to the gIII protein leaving extra nucleotides at the 5′-end of the inserts (Fig. 5). Among the 92 fully sequenced putative mas binding clones, three peptide sequences were repeatedly isolated. The three enriched sequences are: S C R S S S R R Q T (E.seq 1; 44 clones), F L V T L T R T W A I R (E.seq 2; 10 clones), and C M T T Y L R L W R I I (E.seq 3; 2 clones). Interestingly, the three enriched sequences were all from the fifth round of selection, and the enriched sequence 1 clone contained one extra nucleotide in the peptide coding region. On the other hand, alignments of the derived peptide sequences displayed two consensus motifs: R/C-Q/A-A/Q-L-R-R-L-L-R-R/N-G-L/G (consensus motif 1) and W-S-C/P-C/M-S/T-T/S-S/T-T/S-R-S/T-W (consensus motif 2) (Fig. 5). Furthermore, it was noted that the three enriched sequences also aligned with the consensus motif 2 (Fig. 5B).

3.4. *Cell binding characteristics of the isolated phage clones and labeled synthetic peptide*

To assess the specificity of the isolated phage clones, phage binding activity against stable cell lines expressing either mas-GFP or GFP was examined by immunocytochemistry. While only a weak background binding was observed in GFP-expressing control cells (Fig. 6B), a strong punctate surface binding of the phage 3p4A5 (representative phage clone of consensus motif 1) was observed in mas-GFP expressing cells (Fig. 6E). Furthermore, the phage binding also showed strong co-localization with the mas-GFP fluorescence, suggesting the phage binding to mas protein (Fig. 6F). Similar staining patterns were observed with the phage clones 3p4A19, 3p3A31, 3p4A2, 3p4A3, 3p4A10 of consensus motif 1, 3p4A27, 3p5A110 of enriched sequence 1, 3p5A190 of enriched sequence 2, and 3p3A14 of consensus motif 2 (data not shown).

We next determined whether synthetic peptide MBP7 (KAQLRRLS, based on consensus motif 1) displayed a similar binding pattern to isolated clones. After conjugating Alexa Fluor 546 dye to the N-terminus of peptide MBP7, binding characteristics of Alexa Fluor-MBP7 to mas-transfected cells was examined by confocal microscopy. The labeled peptide showed strong binding to CHO Dhfr$^-$ cells transiently expressing mas-GFP but not to cells transiently expressing GFP. Similar to the phage binding, labeled peptide was localized exclusively on the cell surface with punctuate distribution (Fig. 7I). Co-localization of the Alexa Fluor fluorescence and mas-GFP fluorescence was noted, suggesting the binding of labeled peptide to mas-GFP fusion protein (Fig. 7K).

3.5. *Ligand-induced mas internalization*

To determine whether phage clones could bind to and co-localize with mas proteins, MC0M80 cells were incubated with 3p5A190, and cellular distribution of the phage clone and mas proteins were probed with a monoclonal anti-M13 antibody and the polyclonal anti-mas antibody, respectively. To our surprise, significant internalization of phage clone 3p5A190 as well as mas proteins were observed after 10 min incubation with MC0M80 cells (Fig. 8). Moreover, there was a strong co-localization of the internalized phage and mas proteins, indicating the agonist nature of the phage clone and its binding to mas proteins (Fig. 8).

Panning Round	Input Phage (cfu)	Output Phage (cfu)	Input / Output Ratio
I	2.6×10^{12}	8.4×10^{7}	3.0×10^{4}
II	1.3×10^{13}	5.8×10^{7}	2.2×10^{5}
III	3.5×10^{14}	2.2×10^{9}	1.5×10^{5}
IV	6.2×10^{16}	1.5×10^{9}	4.0×10^{7}
V	7.5×10^{16}	3.8×10^{6}	1.9×10^{10}

(A)

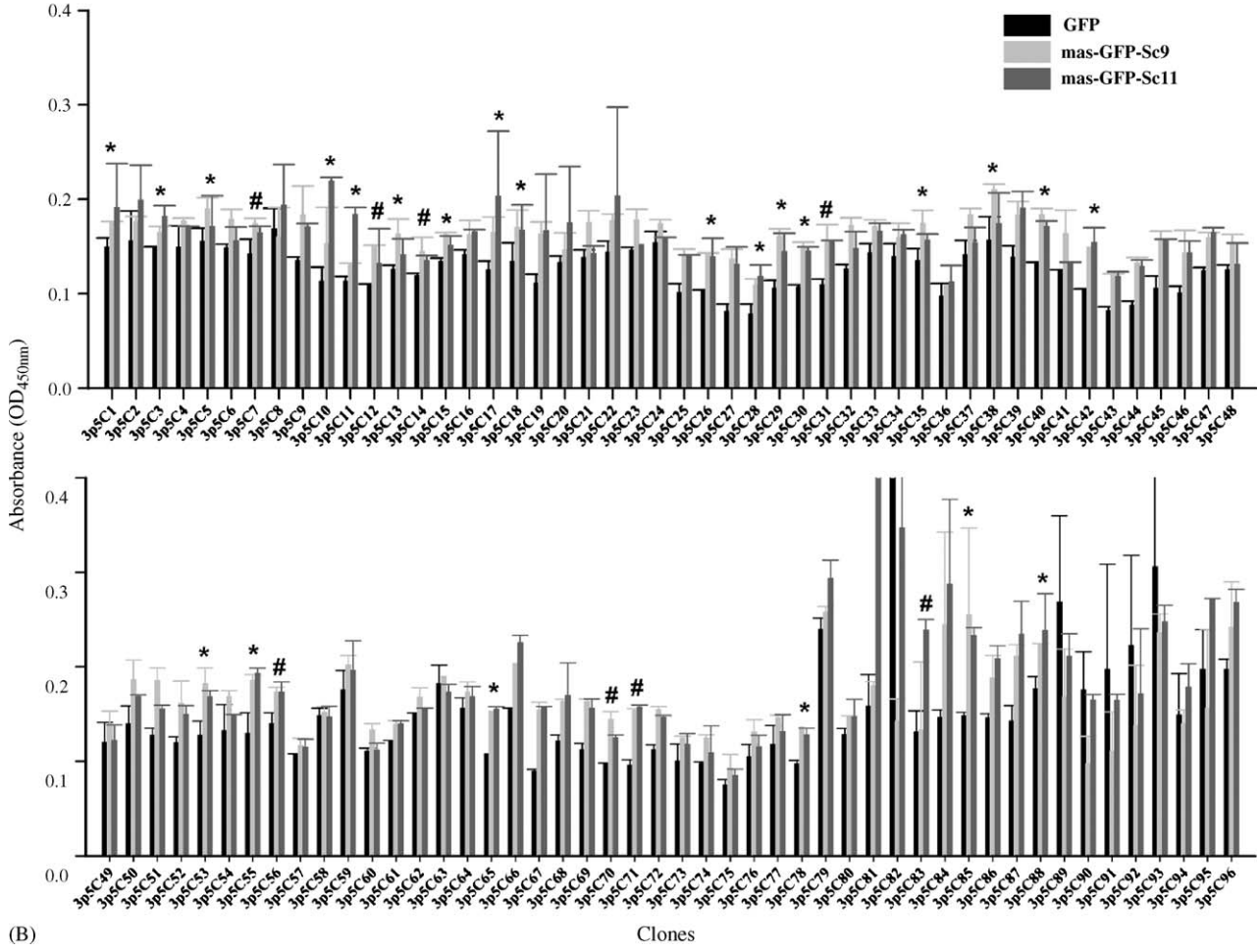

Fig. 4 – Characteristics of mas-specific phage clone selection. (A) Phage titers during the subtractive selection process, showing input and elution titers after each round of panning, are listed. Input phage is the number of phage added to the cells transiently expressing GFP and output phage is the amount of phage eluted from the cells transiently expressing mas-GFP. (B) A representative mas-specific phage clone selection with phageELISA. Phages were prepared from the detergent eluate fraction of the fifth round and analyzed for binding to stable GFP-expressing mas-GFP-Sc9 and mas-GFP-Sc11 cell lines. A robust binding to mas-GFP cell lines by a majority of the clones was observed. The clones marked with '*' represent the phages displaying enriched sequence 1 (E.seq 1) and those marked with '#' represent enriched sequence 2 (E.seq 2).

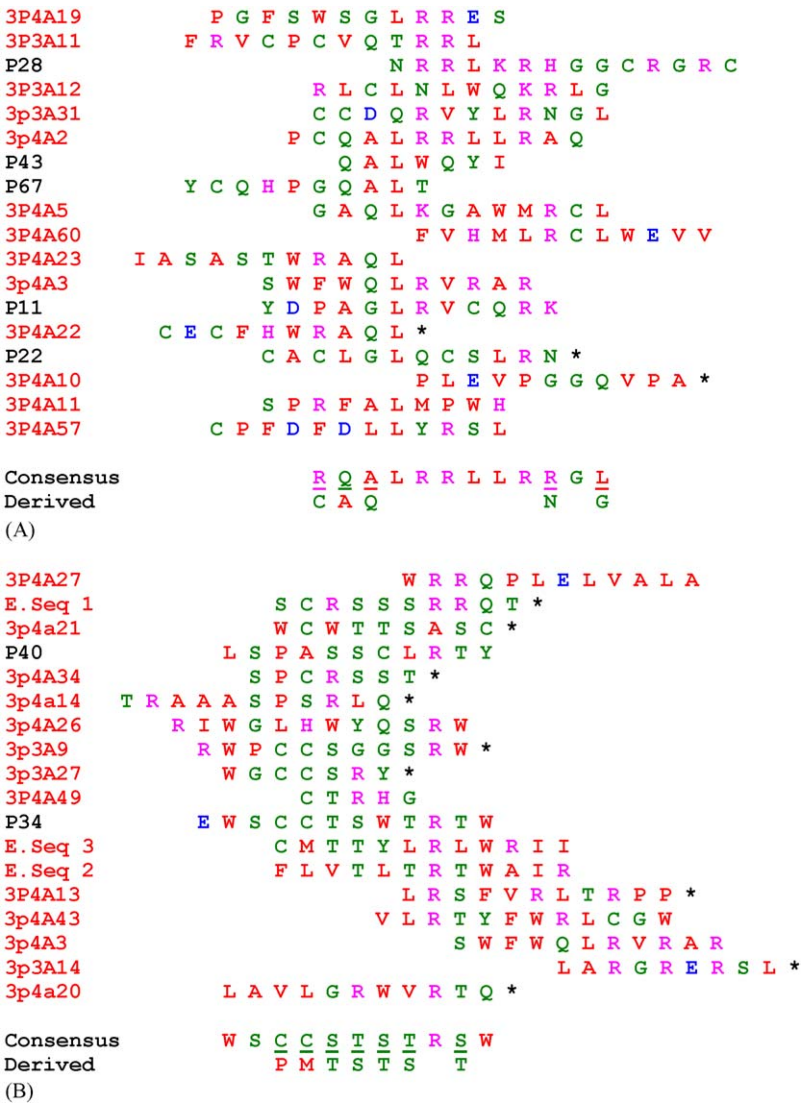

Fig. 5 – Multiple alignments of peptide sequences encoded in the mas-specific phage clones. (A) Peptide sequences of 18 phage clones and the derived consensus motif 1. (B) Peptide sequences of 71 phage clones and the derived consensus motif 2. The peptides were aligned based on the physio-chemical properties of amino acids. The clones colored in black originated from the library screened against MC0M80 cells while the clones colored in red originated from the library screened against cells transiently expressing (24 h) mas-GFP fusion protein. The color codes for the amino acids are: red for non-polar, green for uncharged polar, blue for charged polar and pink for basic amino acids. Asterisk indicates phage clones with one or two extra nucleotides in the insert and the peptide sequence which were translated in frame with respect to phage gIII protein. (For interpretation of the references to color in this figure legend, the reader is referred to the web version of the article.)

Consistent with the internalization of 3p5A190, incubation of MC0M80 with 10 μM MBP7 for 15 min resulted in internalization of the mas protein as revealed by the punctate intracellular staining of mas proteins (Fig. 9D). In the absence of MBP7, antibody staining was detected predominantly on the cell surface (Fig. 9A).

3.6. *MBP7-mediated activation of phospholipase C*

Mas has been shown to be an activator of phospholipase C (PLC) [17,18]. To determine whether MBP7 acts as an agonist of mas and stimulates inositol phosphate production, MC0M80 cells pre-labeled with [^{3}H]-inositol were incubated with MBP7 for 1 h and accumulation of [^{3}H]-inositol phosphates was measured. Activation of the endogenously expressed P2Y purinergic receptor in CHO cells by ATP was used as a positive control. Indeed, ATP (100 μM) induced a significant increase in the [^{3}H]-inositol phosphates in all three cell lines (Fig. 10). Intriguingly, the ATP-induced increase in [^{3}H]-inositol phosphate levels were different in the three cell lines. While the responses to ATP were similar in wild-type and VC0M80 controls, the responses of the MC0M80 cells was only 50% that of the wide-type and VC0M80 cells. MBP7 (10 μM) significantly stimulated [^{3}H]-

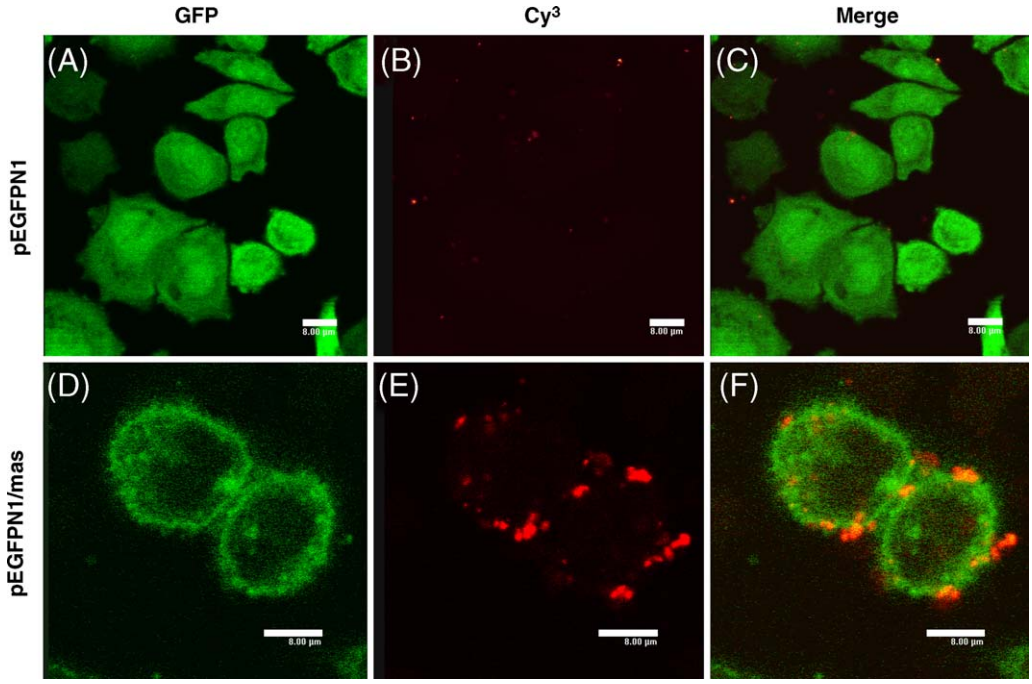

Fig. 6 – (A–F) Cell binding characteristics of the phage clone 3p4A5. Recombinant phage from the clone 3p4A5 was rescued and immunostaining was performed as described in Section 2. Confocal imaging showed a strong, punctate staining of the phage on the cell surface of mas-GFP expressing cells (panel E). Distributions of mas-GFP and phages are represented by green and red pseudo-colors, respectively. Co-localization of mas-GFP and phage is represented as yellow pseudo-color in the images (panel F). The phage staining was specific to mas-GFP expressing cells as there was no staining detected in the GFP expressing cells (panel B). Data shown represent two to four independent experiments with similar results. Scale bar, 8 μm. (For interpretation of the references to color in this figure legend, the reader is referred to the web version of the article.)

inositol phosphate accumulation only in MC0M80 cells (Fig. 10C; $p < 0.05$, one-way ANOVA, $n = 5$), but not in the wild-type and VC0M80 cells (Fig. 10A and B). The increase in the [^{3}H]-inositol phosphates suggests that the MBP7 peptide is an agonist of GPCR mas and Gq is the candidate G protein following mas activation. By contrast, angiotensin-(1-7) (Ang 1-7; 10 μM), which was reported to be the endogenous ligand of mas [19], showed no significant stimulatory affect in MC0M80 cells (Fig. 10C) or in the wild-type and VC0M80 cells (Fig. 10A and B). The stimulatory effect of MBP7 and ATP in mas transfected MC0M80 cells was additive and was significantly different from the responses in the absence of any peptides and in the presence of Ang 1-7 (Fig. 10C), suggesting that there is no cross-talk between mas and P2Y receptors.

To estimate the potency of MBP7 to activate mas, mas over-expressing MC0M80 cells were incubated with increasing concentrations of MBP7. MBP7 produced a log concentration-dependent activation of PLC with an EC_{50} value of 36.41 ± 5.41 μM ($n = 3$), and a Hill slope value significantly greater than unity (2.82 ± 0.06, $p < 0.05$, $n = 3$) (Fig. 11), suggesting a possible co-operative binding of MBP7 to mas. ATP also produced a log concentration-dependent increase in [^{3}H]-inositol phosphate accumulation with an EC_{50} value of 6.82 ± 2.88 μM ($n = 3$) and a Hill slope value not significantly different from unity (1.41 ± 0.52, $n = 3$) (Fig. 11). Although MBP7 was about 6-fold less potent than ATP in activating PLC, the maximal [^{3}H]-inositol phosphate accumulation stimulated by MBP7 at 100 μM was 7.78-fold higher than that of ATP (14,230 ± 1098 and 1828 ± 323 dpm, $n = 3$, for MBP7 and ATP, respectively).

GPCRs such as angiontensin AT_1 and purinergic P2Y receptors are desensitized following agonist stimulation [20]. To examine whether mas would undergo agonist-dependent desensitization, MC0M80 cells were initially exposed to 20 μM MBP7, and 10 min later were further challenged with additional dose of MBP7. It is of interest to note that MBP7-stimulated [^{3}H]-inositol phosphate accumulation was further increased, rather than decreased, by prior exposure of MC0M80 cells to 20 μM MBP7 (Fig. 12).

3.7. *MBP7-stimulated intracellular calcium mobilization*

The changes of intracellular free calcium level ($[Ca^{2+}]_i$) in response to 100 μM MBP7 were compared between transfected and non-transfected CHO cells. Addition of 100 μM MBP7 did not elicit any discernible increase in $[Ca^{2+}]_i$ whereas subsequent addition of 100 μM ATP caused an increase in $[Ca^{2+}]_i$ ($\Delta_{ratio} = 2.27 \pm 0.24$, $n = 3$) in wild-type CHO cells (Fig. 13A). Similar results were obtained in cells transfected with the empty vector alone, thus, the VC0M80 cells only responded to ATP ($\Delta_{ratio} = 2.34 \pm 0.66$, $n = 3$) but not to MBP7 (Fig. 13B). By contrast, the mas over-expressing MC0M80 cells showed an initial increase in $[Ca^{2+}]_i$ ($\Delta_{ratio} = 1.62 \pm 0.29$, $n = 5$) in response

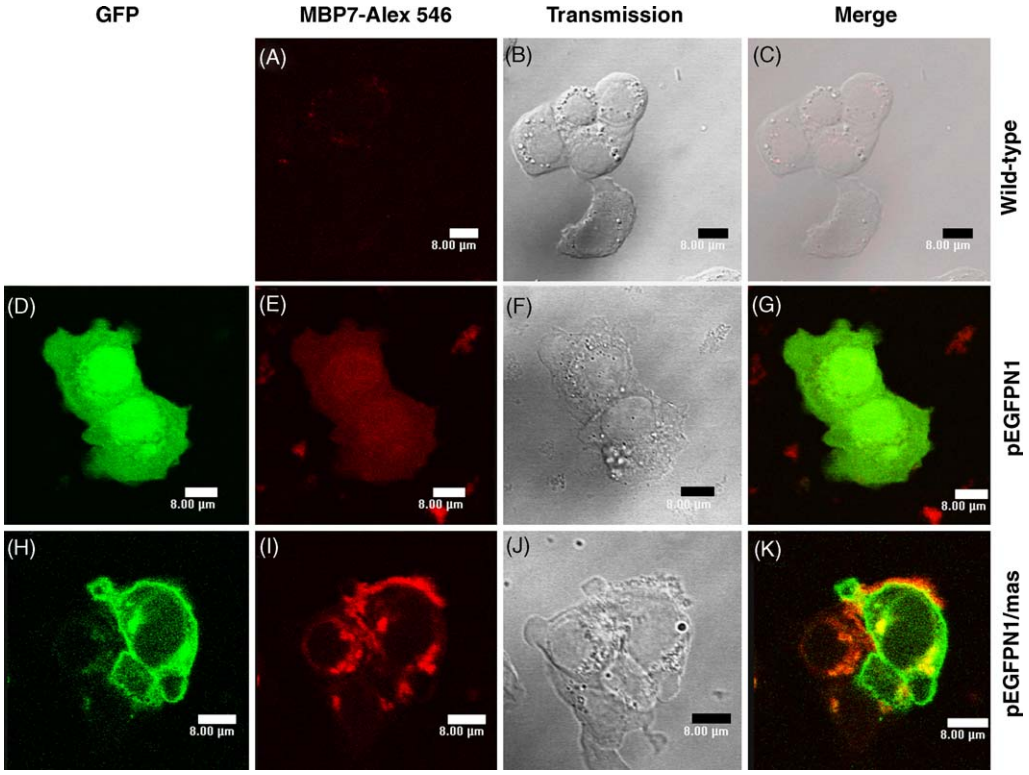
GFP
MBP7-Alex 546
Transmission
Merge
Wild-type
pEGFPN1
pEGFPN1/mas
(A)
(B)
(C)
(D)
(E)
(F)
(G)
(H)
(I)
(J)
(K)
8.00 μm

Fig. 7

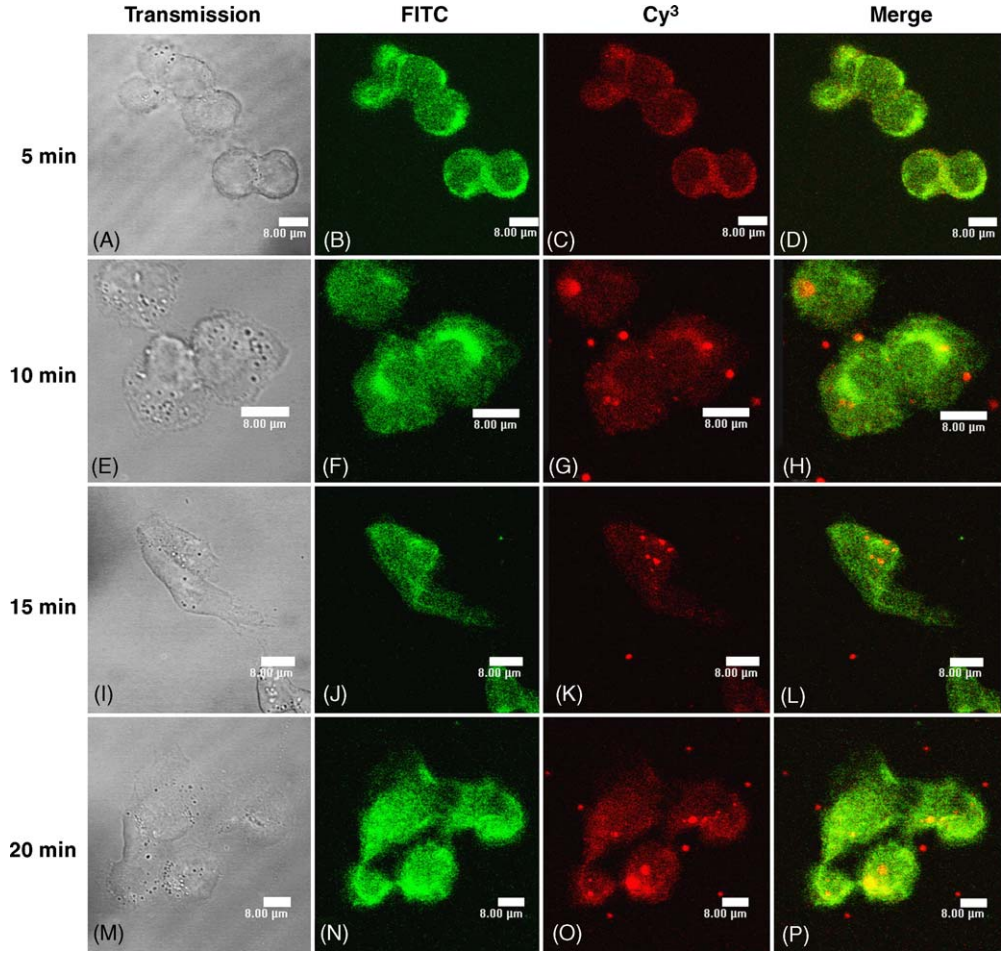
Transmission
FITC
Cy3
Merge
5 min
10 min
15 min
20 min
(A)
(B)
(C)
(D)
(E)
(F)
(G)
(H)
(I)
(J)
(K)
(L)
(M)
(N)
(O)
(P)
8.00 μm

Fig. 8

to 100 μM MBP7 which then decreased to a plateau level. Furthermore, MC0M80 cells still responded to a second challenge with MBP7 added 10 min later, although the change in fluorescence ratio was reduced to 0.45 ± 0.21 (Fig. 13C).

4. Discussion

Mas oncogene was identified more than a decade ago and was reported to be expressed in abundance in the brain and testis. However, understanding its physiological roles has been severely hampered due to lack of information regarding its cognate/surrogate ligands. In order to obtain a pharmacological/surrogate ligand, we used a phage library displaying linear random peptide epitopes (11–16 amino acids) to identify surrogate peptide ligands for this orphan receptor. Alignment of the peptide sequences derived from those putative mas ligands revealed two consensus sequences: R/C-Q/A-A/Q-L-R-R-L-L-R-R/N-G-L/G (consensus motif 1) and W-S-C/P-C/M-S/T-T/S-S/T-T/S-R-S/T-W (consensus motif 2). Furthermore, panning the phage-displayed random peptide library against MC0M80 cells identified several putative mas ligands (P28, P43, P67, P11, P22, P40, P34; Fig. 5) which showed similar peptide motifs as those obtained by screening using mas-GFP expressing cells.

The two consensus sequences obtained are quite different from each other. Consensus motif 1 consists of two LRR motifs separated by a leucine, and is dominated by charged amino acids (arginine and lysine). In contrast, consensus motif 2 consists of a set of polar amino acids flanked by tryptophan. This suggests that peptides representing the two consensus sequences might bind at different sites on mas. It has been previously reported that GPCR mas was poorly activated by FLRF amide peptide [21]. Interestingly several peptides with LR motifs (consensus motif 1) were isolated in the present study, suggesting that the weak response observed with FLRF amide is probably due to the LR motif.

The identified consensus motifs showed no homology to any known peptide hormones, neurotransmitters and other biologically important peptides. However, BLAST query (NCBI, blastp for short nearly exact matches) of the consensus motifs revealed partial homology with different classes of proteins (Table 1). It is of interest to note that the C-terminal tail of mouse olfactory receptor 19, also known as M12 odorant receptor, contains the core sequence 'ALRRLLRR' of consensus motif 1. Human chemokine receptor 10 (CCR10), also known as human G protein-coupled receptor 2 (GPCR2), showed a consensus motif 1-like sequence of 'RQDLRRLLR' at its C-terminus. Both the chemokine and olfactory receptors are members of the GPCR superfamily and the receptors are expressed abundantly along with mas in testis [3,22,23]. Cell surface expression of GPCRs may depend on the formation of heterodimers, as originally demonstrated for the $GABA_B$ receptor [24], and more recently for the olfactory receptor M71 and the β_2-adrenergic receptor [25]. In addition, lines of evidence indicate that formation of GPCR homo- and/or heterodimers is required for mediating hormonal signals [26–28]. Our results suggest that the olfactory receptor 19 and CCR10 may interact with mas in testis.

Perhaps a more plausible protein partner for mas would be CCL27, also known as ALP/ESkine/ILC, which is a ligand for CCR10 and is also abundantly expressed in testis [29–31]. CCL27 possesses the consensus motif 1-like sequence of 'RQPLPSRLLRR', hence we speculate that CCL27 may influence mas receptor activation, and that MBP7 may have an effect on CCR10 and olfactory receptor 19 activity.

Other than GPCRs, consensus motif 1-like peptide sequences were also noted in a putative monosaccharide transporter 1 (ALRRLLRR) and an intestinal facilitative glucose transporter 7 (RQALRRLRG). An increase in the uptake of glucose or translocation of glucose transporter to the plasma membrane in cells stimulated with other GPCR ligands, such as endothelin [32], fMLP or PAF [33], ATP [34] or GLP-2 [35] has been reported. These results suggest that mas might interact directly with the glucose transporters and might contribute to the oncogenic property of mas by regulating cellular uptake of glucose.

In addition, consensus motif-like peptide sequences were also found in various cytosolic proteins, including enzymes for oxidation–reduction reactions, DNA binding proteins helicase and harpin binding protein, as well as transcription factor iroquois (Table 1). However, the possibility that the extra-

Fig. 7 – Binding characteristics of MBP7 on transfected cells transiently expressing mas-GFP. Alexa Fluor 546-labeled MBP7 was added to wild-type CHO Dhfr$^-$ cells (A–C), cells transfected with pEGFP-N1 (D–G) or pEGFP-N1/mas (H–K) as described in Section 2. After 24 h of transfection, cells were exposed to Alexa Fluor 546-labeled MBP7 at 37 °C for 30 min and fluorescent cell images were captured with confocal microscopy. Distributions of mas-GFP and Alexa Fluor 546-labeled MBP7 are represented by green and red pseudo-colors, respectively. The binding of the peptide was specific to mas-GFP expressing cells (panel I) and co-localization with mas-GFP is represented by the yellow pseudo-color (panel K). Background binding was low in wild-type CHO Dhfr$^-$ cells and cells expressing pEGFP-N1. The data shown represent two to four independent experiments with similar results. Scale bar, 8 μm.

Fig. 8 – (A–P) Co-internalization of the phage (3p5A190) and mas proteins. The mas over-expressing MC0M80 cells were challenged with $\sim 2.5 \times 10^{12}$ phage particles (3p5A190, a clone of enriched sequence 2) for the indicated periods. Cellular locations of mas and the phage were detected by immunostaining with respective antibodies. Distributions of mas and phages are represented by green and red pseudo-colors, respectively. Co-localization of mas and phage is represented as yellow pseudo-color in the images. Internalization of the mas and the phage were time-dependent. Internalized mas and phage were found to be co-localized. Data shown represent two to four independent experiments with similar results. Scale bar, 8 μm.

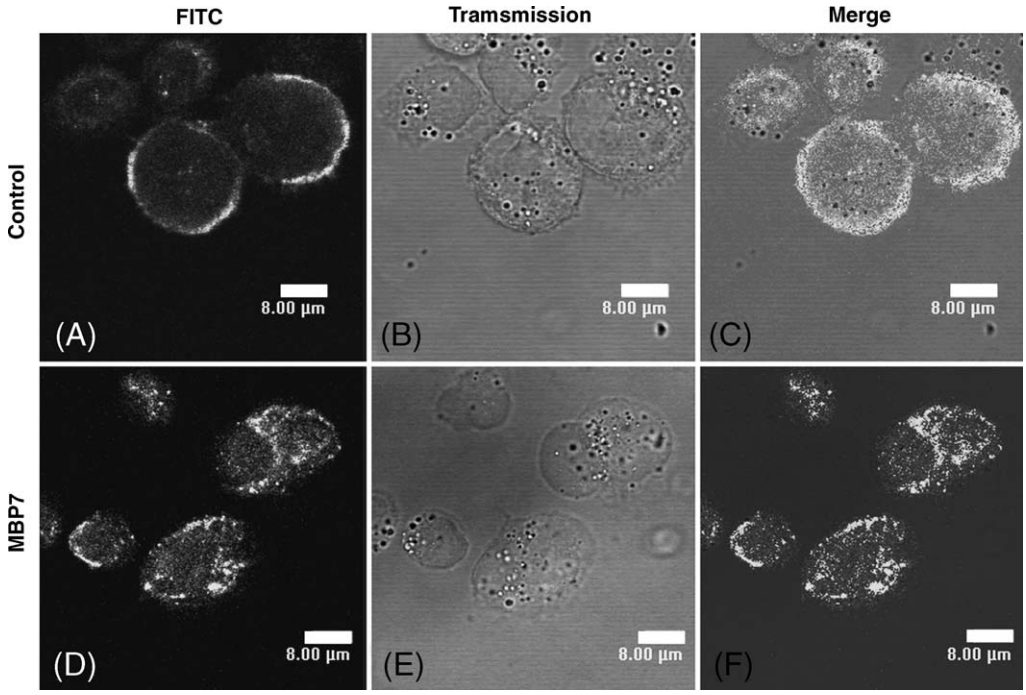

Fig. 9 – (A–F) MBP7-induced internalization of mas proteins. The mas over-expressing MC0M80 cells were stimulated with 10 μM MBP7 (D–F) for 15 min and the mas protein was localized with the mas-specific polyclonal antibody after fixation and permeabilization. MBP7 induced internalization of mas receptor in MC0M80 cells (panel D) while no such internalization was observed in untreated MC0M80 cells (panel A). Data shown represent two to four independent experiments with similar results. Scale bar, 8 μm.

cellular binding pocket of mas interacts with these intracellular proteins is slim.

Homology was also noted between consensus motif 2 and envelope protein of foamy virus (Table 1). In a transgenic mouse model in which foamy virus structural genes were expressed, a severe neurological syndrome developed in transgenic mice at the age of 6–8 weeks old. Histological examination shows high expression of foamy virus transgene in hippocampal neurons [36] where mas has been demonstrated to be highly expressed [37], raising the possibility that mas might serve as a viral receptor for foamy virus.

Specificity of putative mas ligands was confirmed herein by phage immunocytochemistry. The isolated phage clones bound more favorably to cells stably expressing mas-GFP than to control cells stably transfected with vector only. In contrast to the even distribution of mas-GFP protein on the cell surface, the binding of the phages showed a punctate distribution. The processes underlying such punctate distribution of mas ligands is unknown, but similar phage binding patterns have been reported in a study of phage-displayed antibody against epidermal growth factor receptor (EGFR) [38]. On the other hand, the internalization of mas in MC0M80 cells suggests that the phage-displayed peptides acted as agonists of mas. Agonist-activated endocytosis of GPCRs is mediated via clathrin-coated pits [39,40]. Hence, the punctate distribution of phage staining may result from the movement of phage–mas protein complex to clathrin-coated pits prior to receptor endocytosis.

When mas-specific phage clones and the synthetic peptide MBP7 bound to cells stably expressing mas-GFP proteins, the ligand–mas complex remained on the cell surface throughout the experiment. In contrast, the mas proteins were rapidly internalized in MC0M80 cells upon incubation with phage clones or synthetic peptide MBP7. The difference in behavior of the two cell lines strongly suggest an affect of the GFP tag on mas trafficking. GPCRs couple to various interacting proteins such as arrestins and PDZ proteins upon activation to regulate receptor trafficking and relay receptor signals [41–44]. After agonist binding, many GPCRs are phosphorylated on multiple residues in their C-terminal tail by GPCR kinases [45,46], and the agonist-induced receptor internalization is critically dependent on the C-terminal tail [47–51]. These results suggest that GFP tagging to the C-terminus of mas impairs the interaction with receptor interacting proteins to the C-terminal tail of mas and thereby prevents its internalization. Interestingly, a closely related gene of mas, namely the mas related gene (MRG), did not show any affect of GFP tagging on receptor internalization [52]. One possible explanation is that the putative C-terminal tail of MRG is 18-amino-acid longer than that of mas [53], which provides greater flexibility for interaction with different proteins.

Consistent with the internalization studies, the peptide MBP7 induced significant accumulation of [^{3}H]-inositol phosphates, suggesting that MBP7 is an agonist of GPCR mas. Moreover, the additive effect on [^{3}H]-inositol phosphate accumulation stimulated by MBP7 and ATP in mas over-expressing MC0M80 cells suggests that there is no cross-

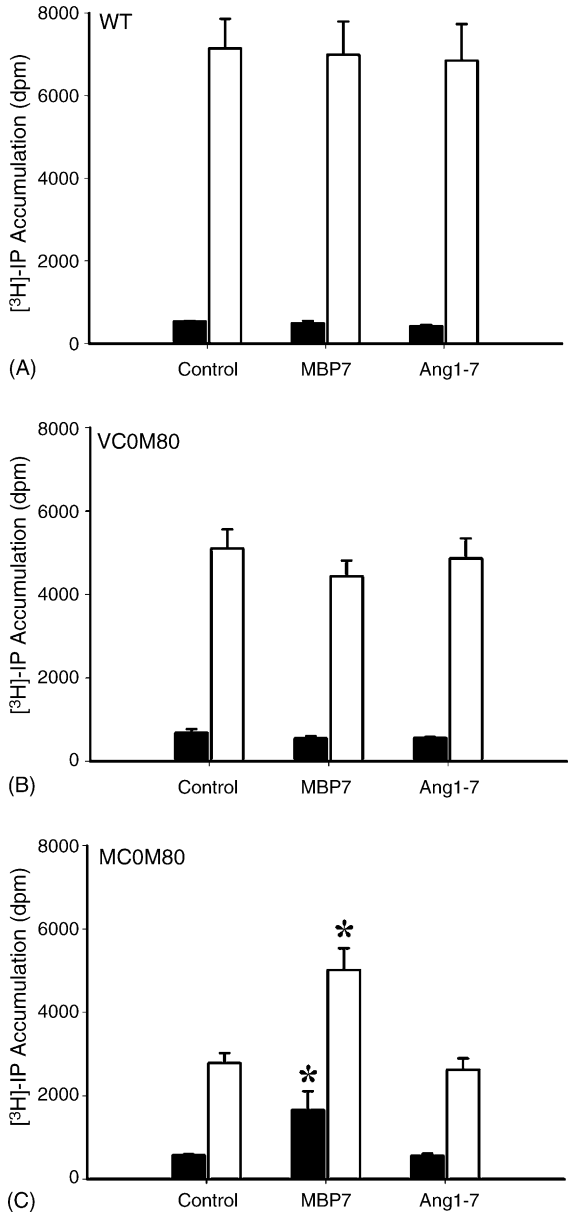

Fig. 10 – MBP7-induced [^{3}H]-inositol phosphate accumulation. Wild-type CHO Dhfr$^-$ (A), vector-transfected VC0M80 (B), and mas over-expressing MC0M80 (C) cells pre-labeled with [^{3}H]-inositol were incubated with 10 μM peptides in the presence (open column) or absence (closed column) of 100 μM ATP. [^{3}H]-Inositol phosphate accumulation was determined as described in Section 2. $^*p < 0.05$, indicating significant accumulation of [^{3}H]-inositol phosphates in MC0M80 cells stimulated with 10 μM MBP7 in the absence (closed column) or presence (open column) of 100 μM ATP in comparison with the respective control. Data were analyzed with Kruskal–Wallis analysis of variance on ranks using SigmaStat (Version 3.1, SPSS Inc., Chicago, IL, USA). Data are means ± S.E.M. of four to five independent experiments with duplicate samples.

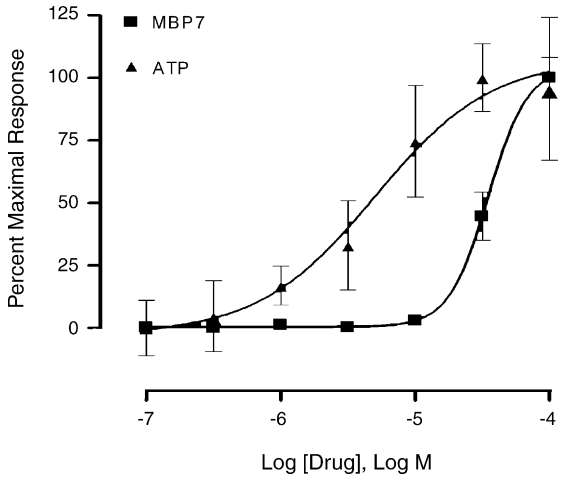

Fig. 11 – Log concentration-dependent stimulation of [^{3}H]-inositol phosphate accumulation by MBP7. MC0M80 cells pre-labeled with [^{3}H]-inositol were incubated with MBP7 (■) or ATP (▲) at the indicated concentrations. [^{3}H]-Inositol phosphate accumulation was determined as described in Section 2. Individual data set was normalized against the corresponding maximal responses which were expressed as 100%. Normalized data sets were curve fitted with non-linear regression using Prism 4. Data are means ± S.E.M. of three independent experiments with duplicate samples.

talk between mas and the P2Y receptor, and the two types of receptor are activated independently. However, the reason for the decrease of ATP-stimulated [^{3}H]-inositol phosphate accumulation in MC0M80 cells compared to the control cells

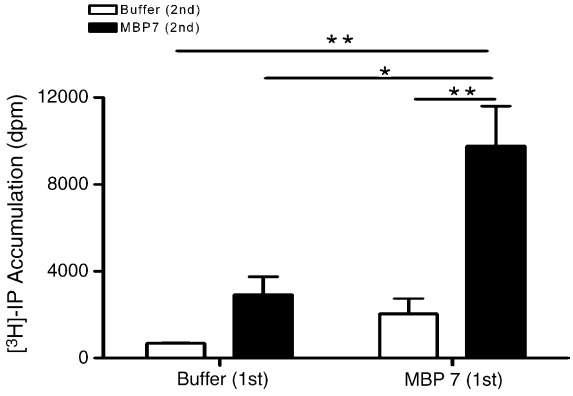

Fig. 12 – Effect of repeated MBP7 stimulation on [^{3}H]-inositol phosphate accumulation. MC0M80 cells pre-labeled with [^{3}H]-inositol were first incubated in the absence (buffer only) or presence of 20 μM MBP7. After 10 min incubation, the cells were challenged with buffer only (open column) or 20 μM MBP7 (close column). [^{3}H]-Inositol phosphate accumulation was determined as described in Section 2. Significant differences between groups are indicated as $^*p < 0.05$ and $^{**}p < 0.01$. Data were analyzed with Bonferroni's multiple comparison test using Prism 4. Data are means ± S.E.M. of three independent experiments with triplicate samples.

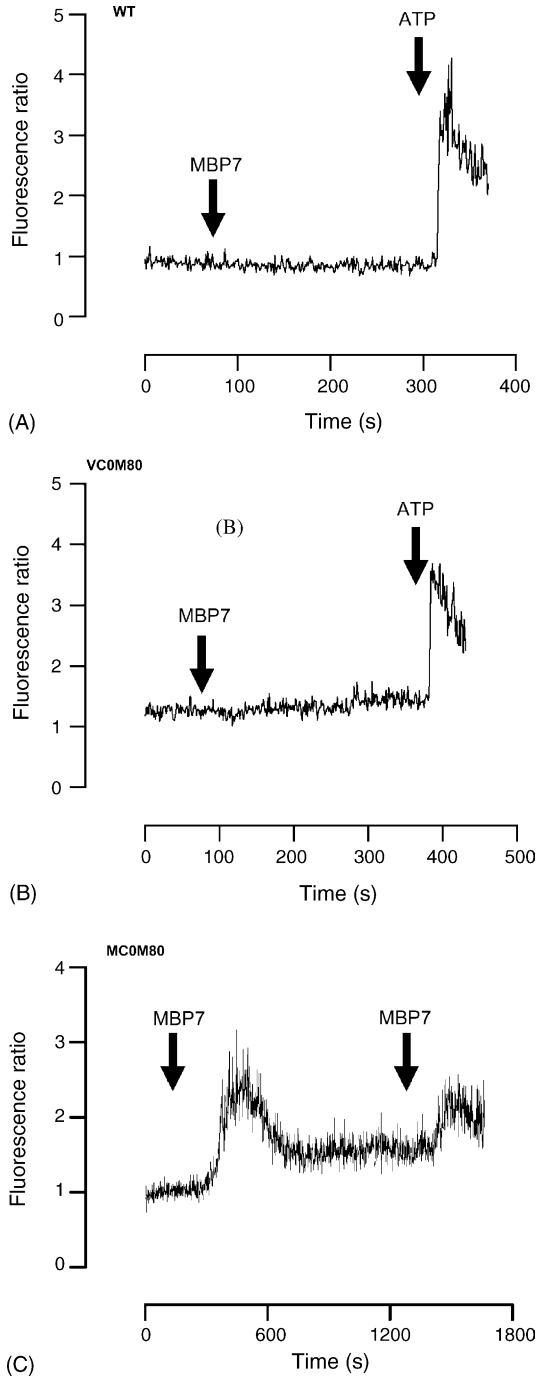

Fig. 13 – Effect of MBP7 on $[Ca^{2+}]_i$. Wild-type CHO Dhfr$^-$ (A), vector-transfected VC0M80 (B), and mas over-expressing MC0M80 (C) cells were loaded with Fura-2/AM in the presence of pluronic F127 for 45 min. Cells were stimulated with 100 μM MBP7 or ATP as indicated by the arrows, and changes in Fura-2 fluorescence were measured as described in Section 2. The results are expressed as Fura-2 fluorescence ratio (340/380 nm). Data shown are representative of three to five separate measurements.

is unknown. The basal PLC activity was similar in the control and mas over-expressing cells, thus the decrease in [^{3}H]-inositol phosphate production may result from a decrease in P2Y receptor expression in MC0M80 cells. Mas has been reported to form a constitutive hetero-oligomeric complex with angiotensin AT_1 receptors which results in inhibition of angiotensin II-induced increase in $[Ca^{2+}]_i$ and inositol phosphates [54]. Therefore, mas may additionally form a hetero-oligomeric complex with purinergic P2Y receptors, which results in an attenuation of ATP-induced stimulation of PLC. Alternatively, despite the lack of direct evidence, the presence of preformed receptor-G protein complexes has been suggested [55–57]. Hence, the possibility exists that over-expression of mas causes a re-distribution of the endogenous pool of Gq between the various GPCRs in cells, resulting in a lower response to a specific ligand such as ATP.

Although the calcium mobilization response to MBP7 in mas over-expressing MC0M80 cells was reduced by 70% by prior exposure to MBP7, there was no evidence of mas desensitization when assaying [^{3}H]-inositol phosphate accumulation. Such differential desensitization of calcium and inositol phosphate responses has been reported also for gonadotropin-releasing hormone receptors [58] and bradykinin B1 receptors [59]. In comparison with ATP, MBP7 produced a much steeper log concentration-dependent response curve for [^{3}H]-inositol phosphate accumulation, suggesting the possibility of co-operative activation of mas by MBP7. These results revel a distinct pharmacological profile for MBP7-stimulated mas, and further studies are necessary to examine the effects on mas signaling of mas over-expression by methotrexate-induced gene amplification.

It has previously been reported that mas encodes a functional angiotensin receptor based on an increase of intracellular calcium levels in response to angiotensins in Xenopus oocytes transiently expressing mas [60]. In a mas-deficient mouse model, the binding of Ang 1-7 to kidney [19] and Ang 1-7-induced enhancement of LTP in hippocampus [61] are abolished, therefore Ang 1-7 has been suggested to be the endogenous ligand of mas. However, mas only shares an overall 8 and 19% amino acid identity with the cloned angiotensin AT_1 and AT_2 receptors, respectively [62,63]. In addition, the angiotensin-induced calcium responses in mas-transfected cells were dependent on endogenous expression of angiotensin receptors [64]. Recently, mas has been demonstrated to form an inhibitory complex with angiotensin AT_1 receptors [54]. In addition, Ang 1-7 mediates its vasodepressor effect [65] and its inhibitory effect on Na^+-ATPase [66] via the angiotensin AT_2 receptors. In the present study, the peptides identified showed no homology with angiotensin or its derivatives. In contrast to MBP7, Ang 1-7 did not stimulate [^{3}H]-inositol phosphate accumulation in mas over-expressing MC0M80 cells. These findings suggest that mas might play a significant role in mediating cellular responses to angiotensins, but the nature of this mas-angiotensin interaction has yet to be resolved.

In conclusion, we have identified a surrogate peptide agonist for mas by using a phage-displayed random peptide library. In addition, with mas as an example, we have also demonstrated a systematic way to probe orphan GPCRs and

Table 1 – Proteins consisting of peptide sequences that shared homology with the mas-binding consensus motifs

Protein class	Consensus motif 1 (RQALRRLLRRGL)		Consensus motif 2 (WSCCSTSTRSW)	
	Protein	Accession number	Protein	Accession number
Enzymes and regulatory proteins	Kidney and liver proline oxidase	XP_541686.1	NADH dehydrogenase I, G subunit	NP_954479.1
	Fe-S oxidoreductase	NP_614215.1	Phosphogluconate dehydratase	ZP_00111575
	Pristinamycin I synthetase	CAA67140.1	Alpha mannosidase II	BAA09510.1
	Superfamily II DNA and RNA helicases	ZP_00270322.1	Harpin binding protein	AAR26487
	ATP-dependent DNA helicase	YP_147039.1	Iroquois 4a protein	AAW34337
	Putative acyltransferase	YP_145344.1		
Membrane proteins	Putative monosaccharide transporter 1	XP_466377.1		
	Intestinal facilitative glucose transporter 7	NP_997303.1		
G protein-coupled receptors	Olfactory receptor 19	NP_666447.1		
	Olfactory receptor MOR256-16	XP_605585		
	CC chemokine receptor 10	NP_057686.1		
	G protein-coupled receptor 2	AAF72871.1		
Viral coat proteins			Envelope protein-bovine foamy virus	AAN08117.1
			Envelope protein-simian foamy virus	AAA47794.1

The mas-binding consensus motif sequences were subjected to BLAST search against NCBI databases using the Blastp program for short nearly exact matches to identify homologous proteins. Only proteins that displayed a peptide sequence longer than eight amino acids which showed a homology larger than 80% with the consensus motifs were classified and represented in the table.

identify new pharmacological tools to further enhance our understanding of these orphan receptors.

Acknowledgements

Special thanks to Dr. David R. Poyner for his critical comments and helpful suggestions on the project. The authors also would like to thank the excellent technical help of Kevin B.S. Chow, Helen S.N. Tsai, Denis T.M. Ip, and Wallace Yip. This work was supported in part by an RGC Direct Grant (2330-140) to WTC.

REFERENCES

[1] Chalmers DT, Behan DP. The use of constitutively active GPCRs in drug discovery and functional genomics. Nat Rev Drug Discov 2002;1:599–608.
[2] Young D, Waitches G, Birchmeier C, Fasano O, Wigler M. Isolation and characterization of a new cellular oncogene encoding a protein with multiple potential transmembrane domains. Cell 1986;45:711–9.
[3] Alenina N, Baranova T, Smirnow E, Bader M, Lippoldt A, Patkin E, et al. Cell type-specific expression of the Mas proto-oncogene in testis. J Histochem Cytochem 2002;50:691–6.
[4] Bunnemann B, Fuxe K, Metzger R, Mullins J, Jackson TR, Hanley MR, et al. Autoradiographic localization of mas proto-oncogene mRNA in adult rat brain using in situ hybridization. Neurosci Lett 1990;114:147–53.
[5] van 't Veer LJ, van den Berg-Bakker LA, Hermens RP, Deprez RL, Schrier PI. High frequency of mas oncogene activation detected in the NIH3T3 tumorigenicity assay. Oncogene Res 1988;3:247–54.
[6] Janssen JW, Steenvoorden AC, Schmidtberger M, Bartram CR. Activation of the mas oncogene during transfection of monoblastic cell line DNA. Leukemia 1988;2:318–20.
[7] Smith GP. Filamentous fusion phage: novel expression vectors that display cloned antigens on the virion surface. Science 1985;228:1315–7.
[8] Spear MA, Breakefield XO, Beltzer J, Schuback D, Weissleder R, Pardo FS, et al. Isolation, characterization, and recovery of small peptide phage display epitopes selected against viable malignant glioma cells. Cancer Gene Ther 2001;8:506–11.
[9] Houimel M, Loetscher P, Baggiolini M, Mazzucchelli L. Functional inhibition of CCR3-dependent responses by peptides derived from phage libraries. Eur J Immunol 2001;31:3535–45.
[10] Szardenings M, Tornroth S, Mutulis F, Muceniece R, Keinanen K, Kuusinen A, et al. Phage display selection on whole cells yields a peptide specific for melanocortin receptor 1. J Biol Chem 1997;272:27943–8.
[11] Yiu AK, Wong PF, Yeung SY, Lam SM, Luk SK, Cheung WT. Immunohistochemical localization of type-II (AT_2) angiotensin receptors with a polyclonal antibody against a peptide from the C-terminal tail. Regul Pept 1997;70:15–21.
[12] Wong PF, Lee SS, Cheung WT. Immunohistochemical colocalization of type II angiotensin receptors with somatostatin in rat pancreas. Regul Pept 2004; 117:195–205.

[13] Chow KB, Wong YH, Wise H. Prostacyclin receptor-independent inhibition of phospholipase C activity by non-prostanoid prostacyclin mimetics. Br J Pharmacol 2001;134:1375–84.
[14] Yue GG, Yip TW, Huang Y, Ko WH. Cellular mechanism for potentiation of Ca^{2+}-mediated Cl^- secretion by the flavonoid baicalein in intestinal epithelia. J Biol Chem 2004;279:39310–6.
[15] MacBeath G, Kast P. UGA read-through artifacts—when popular gene expression systems need a pATCH. Biotechniques 1998;24:789–94.
[16] Carcamo J, Ravera MW, Brissette R, Dedova O, Beasley JR, Alam-Moghe A, et al. Unexpected frameshifts from gene to expressed protein in a phage-displayed peptide library. Proc Natl Acad Sci USA 1998;95:11146–51.
[17] Jackson TR, Hanley MR. Tumor promoter 12-O-tetradecanoylphorbol 13-acetate inhibits mas/angiotensin receptor-stimulated inositol phosphate production and intracellular Ca^{2+} elevation in the 401L-C3 neuronal cell line. FEBS Lett 1989;251:27–30.
[18] Poyner DR, Hawkins PT, Benton HP, Hanley MR. Changes in inositol lipids and phosphates after stimulation of the MAS-transfected NG115-401L-C3 cell line by mitogenic and non-mitogenic stimuli. Biochem J 1990;271:605–11.
[19] Santos RA, Simoes e Silva AC, Maric C, Silva DM, Machado RP, de Buhr I, et al. Angiotensin-(1-7) is an endogenous ligand for the G protein-coupled receptor Mas. Proc Natl Acad Sci USA 2003;100:8258–63.
[20] Sum CS, Wan DC, Cheung WT. Potentiation of purinergic transmission by angiotensin in prostatic rat vas deferens. Br J Pharmacol 1996;118:1523–9.
[21] Dong X, Han S, Zylka MJ, Simon MI, Anderson DJ. A diverse family of GPCRs expressed in specific subsets of nociceptive sensory neurons. Cell 2001;106:619–32.
[22] Jarmin DI, Rits M, Bota D, Gerard NP, Graham GJ, Clark-Lewis I, et al. Cutting edge: identification of the orphan receptor G-protein-coupled receptor 2 as CCR10, a specific receptor for the chemokine ESkine. J Immunol 2000;164:3460–4.
[23] Vanderhaeghen P, Schurmans S, Vassart G, Parmentier M. Specific repertoire of olfactory receptor genes in the male germ cells of several mammalian species. Genomics 1997;39:239–46.
[24] White JH, Wise A, Main MJ, Green A, Fraser NJ, Disney GH, et al. Heterodimerization is required for the formation of a functional $GABA_B$ receptor. Nature 1998;396:679–82.
[25] Hague C, Uberti MA, Chen Z, Bush CF, Jones SV, Ressler KJ, et al. Olfactory receptor surface expression is driven by association with the β_2-adrenergic receptor. Proc Natl Acad Sci USA 2004;101:13672–6.
[26] Breitwieser GE. G protein-coupled receptor oligomerization: implications for G protein activation and cell signaling. Circ Res 2004;94:17–27.
[27] Park PS, Filipek S, Wells JW, Palczewski K. Oligomerization of G protein-coupled receptors: past, present, and future. Biochemistry 2004;43:15643–56.
[28] Park S-HP, Palczewski K. Diversifying the repertoire of G protein-coupled receptors through oligomerization. Proc Natl Acad Sci USA 2005;102:8793–4.
[29] Baird JW, Nibbs RJ, Komai-Koma M, Connolly JA, Ottersbach K, Clark-Lewis I, et al. ESkine, a novel β-chemokine, is differentially spliced to produce secretable and nuclear targeted isoforms. J Biol Chem 1999;274:33496–503.
[30] Hromas R, Broxmeyer HE, Kim C, Christopherson II K, Hou YH. Isolation of ALP, a novel divergent murine CC chemokine with a unique carboxy terminal extension. Biochem Biophys Res Commun 1999;258:737–40.
[31] Ishikawa-Mochizuki I, Kitaura M, Baba M, Nakayama T, Izawa D, Imai T, et al. Molecular cloning of a novel CC chemokine, interleukin-11 receptor alpha-locus chemokine (ILC), which is located on chromosome 9p13 and a potential homologue of a CC chemokine encoded by molluscum contagiosum virus. FEBS Lett 1999;460:544–8.
[32] Wu-Wong JR, Berg CE, Wang J, Chiou WJ, Fissel B. Endothelin stimulates glucose uptake and GLUT4 translocation via activation of endothelin ETA receptor in 3T3-L1 adipocytes. J Biol Chem 1999;274:8103–10.
[33] Hagi A, Hayashi H, Kishi K, Wang L, Ebina Y. Activation of G-protein coupled fMLP or PAF receptor directly triggers glucose transporter type 1 (GLUT1) translocation in Chinese hamster ovary (CHO) cells stably expressing fMLP or PAF receptor. J Med Invest 2000;47:19–28.
[34] Solini A, Chiozzi P, Morelli A, Passaro A, Fellin R, Di Virgilio F. Defective P2Y purinergic receptor function: a possible novel mechanism for impaired glucose transport. J Cell Physiol 2003;197:435–44.
[35] Lovshin J, Drucker DJ. New frontiers in the biology of GLP-2. Regul Pept 2000;90:27–32.
[36] Aguzzi A. The foamy virus family: molecular biology, epidemiology and neuropathology. Biochim Biophys Acta 1993;1155:1–24.
[37] Metzger R, Bader M, Ludwig T, Berberich C, Bunnemann B, Ganten D. Expression of the mouse and rat mas proto-oncogene in the brain and peripheral tissues. FEBS Lett 1995;357:27–32.
[38] Heitner T, Moor A, Garrison JL, Marks C, Hasan T, Marks JD. Selection of cell binding and internalizing epidermal growth factor receptor antibodies from a phage display library. J Immunol Methods 2001;248:17–30.
[39] Shenoy SK, Lefkowitz RJ. Multifaceted roles of beta-arrestins in the regulation of seven-membrane-spanning receptor trafficking and signalling. Biochem J 2003;375:503–15.
[40] von Zastrow M. Mechanisms regulating membrane trafficking of G protein-coupled receptors in the endocytic pathway. Life Sci 2003;74:217–24.
[41] Brady AE, Limbird LE. G protein-coupled receptor interacting proteins: emerging roles in localization and signal transduction. Cell Signal 2002;14:297–309.
[42] Hall RA, Lefkowitz RJ. Regulation of G protein-coupled receptor signaling by scaffold proteins. Circ Res 2002;91:672–80.
[43] Lefkowitz RJ, Shenoy SK. Transductin of receptor signals by β-arrestins. Science 2005;308:512–7.
[44] Trejo J. Internal PDZ ligands: novel endocytic recycling motifs for G protein-coupled receptors. Mol Pharmacol 2005;67:1388–90.
[45] Carman CV, Benovic JL. G-protein-coupled receptors: turn-ons and turn-offs. Curr Opin Neurobiol 1998;8:335–44.
[46] Zhang J, Ferguson SS, Barak LS, Bodduluri SR, Laporte SA, Law PY, et al. Role for G protein-coupled receptor kinase in agonist-specific regulation of mu-opioid receptor responsiveness. Proc Natl Acad Sci USA 1998;95:7157–62.
[47] Drmota T, Milligan G. Kinetic analysis of the internalization and recycling of [^{3}H]TRH and C-terminal truncations of the long isoform of the rat thyrotropin-releasing hormone receptor-1. Biochem J 2000;346(Pt 3):711–8.
[48] Mundell SJ, Pula G, Carswell K, Roberts PJ, Kelly E. Agonist-induced internalization of metabotropic glutamate receptor 1A: structural determinants for protein kinase C- and G protein-coupled receptor kinase-mediated internalization. J Neurochem 2003;84:294–304.
[49] Nussenzveig DR, Heinflink M, Gershengorn MC. Agonist-stimulated internalization of the thyrotropin-releasing hormone receptor is dependent on two domains in the receptor carboxyl terminus. J Biol Chem 1993;268:2389–92.
[50] Paasche JD, Attramadal T, Kristiansen K, Oksvold MP, Johansen HK, Huitfeldt HS, et al. Subtype-specific sorting of the ET_A endothelin receptor by a novel endocytic recycling

signal for G protein-coupled receptors. Mol Pharmacol 2005;67:1581–90.
[51] Swords FM, Baig A, Malchoff DM, Malchoff CD, Thorner MO, King PJ, et al. Impaired desensitization of a mutant adrenocorticotropin receptor associated with apparent constitutive activity. Mol Endocrinol 2002;16:2746–53.
[52] Han SK, Dong X, Hwang JI, Zylka MJ, Anderson DJ, Simon MI. Orphan G protein-coupled receptors MrgA1 and MrgC11 are distinctively activated by RF-amide-related peptides through the $G\alpha_{q/11}$ pathway. Proc Natl Acad Sci USA 2002;99:14740–5.
[53] Monnot C, Weber V, Stinnakre J, Bihoreau C, Teutsch B, Corvol P, et al. Cloning and functional characterization of a novel mas-related gene, modulating intracellular angiotensin II actions. Mol Endocrinol 1991;5:1477–87.
[54] Kostenis E, Milligan G, Christopoulos A, Sanchez-Ferrer CF, Heringer-Walther S, Sexton PM, et al. G-protein-coupled receptor Mas is a physiological antagonist of the angiotensin II type 1 receptor. Circulation 2005;111:1806–13.
[55] Avlani V, May LT, Sexton PM, Christopoulos A. Application of a kinetic model to the apparently complex behavior of negative and positive allosteric modulators of muscarinic acetylcholine receptors. J Pharmacol Exp Ther 2004;308:1062–72.
[56] De Lean A, Stadel JM, Lefkowitz RJ. A ternary complex model explains the agonist-specific binding properties of the adenylate cyclase-coupled β-adrenergic receptor. J Biol Chem 1980;255:7108–17.
[57] Hermans E. Biochemical and pharmacological control of the multiplicity of coupling at G-protein-coupled receptors. Pharmacol Ther 2003;99:25–44.
[58] Anderson L, McGregor A, Cook JV, Chilvers E, Eidne KA. Rapid desensitization of GnRH-stimulated intracellular signalling events in alpha T3-1 and HEK-293 cells expressing the GnRH receptor. Endocrinology 1995;136:5228–31.
[59] Zhou X, Prado GN, Taylor L, Yang X, Polgar P. Regulation of inducible bradykinin B1 receptor gene expression through absence of internalization and resensitization. J Cell Biochem 2000;78:351–62.
[60] Jackson TR, Blair LA, Marshall J, Goedert M, Hanley MR. The mas oncogene encodes an angiotensin receptor. Nature 1988;335:437–40.
[61] Hellner K, Walther T, Schubert M, Albrecht D. Angiotensin-(1-7) enhances LTP in the hippocampus through the G-protein-coupled receptor Mas. Mol Cell Neurosci 2005;29:427–35.
[62] Mukoyama M, Nakajima M, Horiuchi M, Sasamura H, Pratt RE, Dzau VJ. Expression cloning of type 2 angiotensin II receptor reveals a unique class of seven-transmembrane receptors. J Biol Chem 1993;268:24539–42.
[63] Murphy TJ, Alexander RW, Griendling KK, Runge MS, Bernstein KE. Isolation of a cDNA encoding the vascular type-1 angiotensin II receptor. Nature 1991;351:233–6.
[64] Ambroz C, Clark AJ, Catt KJ. The mas oncogene enhances angiotensin-induced $[Ca^{2+}]_i$ responses in cells with pre-existing angiotensin II receptors. Biochim Biophys Acta 1991;1133:107–11.
[65] Walters PE, Gaspari TA, Widdop RE. Angiotensin-(1-7) acts as a vasodepressor agent via angiotensin II type 2 receptors in conscious rats. Hypertension 2005;45:960–6.
[66] De Souza AM, Lopes AG, Pizzino CP, Fossari RN, Miguel NC, Cardozo FP, et al. Angiotensin II and angiotensin-(1-7) inhibit the inner cortex Na^+-ATPase activity through AT_2 receptor. Regul Pept 2004;120:167–75.